PERGAMON

Neural Networks 15 (2002) 689–707

Neural Networks

www.elsevier.com/locate/neunet

2002 Special issue

Neuromodulation, theta rhythm and rat spatial navigation

Michael E. Hasselmo*, Jonathan Hay, Maxim Ilyn, Anatoli Gorchetchnikov

Department of Psychology, Program in Neuroscience, Center for BioDynamics, Boston University, 64 Cummington Street, Boston, MA 02215, USA

Received 31 October 2001; accepted 25 April 2002

Abstract

Cholinergic and GABAergic innervation of the hippocampus plays an important role in human memory function and rat spatial navigation. Drugs which block acetylcholine receptors or enhance GABA receptor activation cause striking impairments in the encoding of new information. Lesions of the cholinergic innervation of the hippocampus reduce the amplitude of hippocampal theta rhythm and cause impairments in spatial navigation tasks, including the Morris water maze, eight-arm radial maze, spatial reversal and delayed alternation. Here, we review previous work on the role of cholinergic modulation in memory function, and we present a new model of the hippocampus and entorhinal cortex describing the interaction of these regions for goal-directed spatial navigation in behavioral tasks. These mechanisms require separate functional phases for: (1) encoding of pathways without interference from retrieval, and (2) retrieval of pathways for guiding selection of the next movement. We present analysis exploring how phasic changes in physiological variables during hippocampal theta rhythm could provide these different phases and enhance spatial navigation function.

Keywords: Entorhinal cortex; GABAergic innervation; Hippocampal theta rhythm

1. Acetylcholine and GABA modulation in the hippocampus

The hippocampus receives extensive cholinergic and GABAergic innervation from the medial septum, which appears important for the role of the hippocampus in human memory function and rat spatial navigation. In humans, blockade of muscarinic acetylcholine receptors by drugs such as scopolamine strongly impairs the encoding of new information but not the retrieval of previously encoded information in verbal memory tasks (Ghoneim & Mewaldt, 1975; Hasselmo, 1995 for review). Similarly, enhancement of GABA receptor responses by benzodiazepine drugs also causes significant encoding impairments in humans (Ghoneim & Mewaldt, 1975). In rats, the muscarinic receptor blocker atropine impairs the encoding of platform location in the Morris water maze (Sutherland, Whishaw, & Regehr, 1982). Acetylcholine levels in the hippocampus are highest when a rat is actively exploring the environment, and lower when the rat sits quietly or performs behaviors such as eating or grooming (Marrosu et al., 1995), as summarized in Fig. 1A. The higher levels of acetylcholine are correlated with theta rhythm oscillations (3–12 Hz) in the hippocampal EEG.

1.1. Acetylcholine may enhance encoding dynamics

Modeling suggests that acetylcholine could set appropriate dynamics for encoding of new information within the hippocampal formation (Hasselmo & Bower, 1993; Hasselmo & Schnell, 1994; Hasselmo & Wyble, 1997). That previous work focused on longer periods of encoding versus retrieval, whereas later sections of this article focus on more rapid transitions between encoding and retrieval dynamics within each cycle of the theta rhythm.

Acetylcholine causes physiological effects appropriate for encoding of new information. Activation of muscarinic acetylcholine receptors enhances the rate of synaptic modification at excitatory feedback connections in the cortex, as seen in experiments showing cholinergic enhancement of long-term potentiation (Hasselmo & Barkai, 1995; Huerta & Lisman, 1993; Patil, Linster, Lubenov, & Hasselmo, 1998). At the same time as it enhances long-term potentiation (LTP), acetylcholine suppresses excitatory synaptic transmission at feedback synapses (Hasselmo & Bower, 1993; Hasselmo & Schnell, 1994), while leaving excitatory feedforward synapses relatively unaffected. Thus, feedback synapses have weak

* Corresponding author. Tel.: +1-617-353-1397; fax: +1-617-353-1424.
E-mail addresses: hasselmo@bu.edu (M.E. Hasselmo)

0893-6080/02/$ - see front matter
PII: S0893-6080(02)00057-6

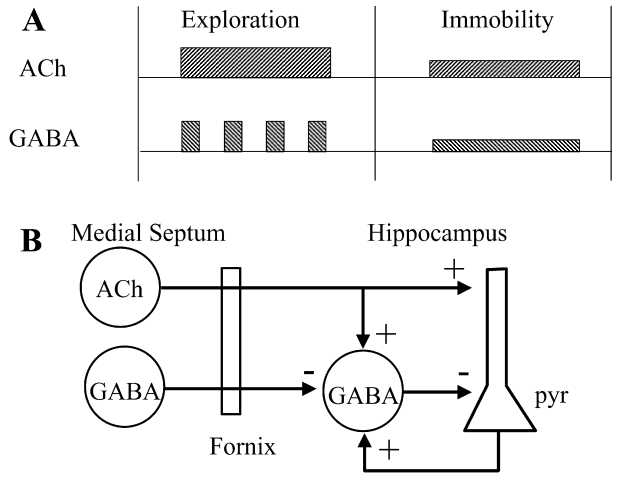

Fig. 1. (A) Neuromodulatory changes in the hippocampus during movement through the environment and during immobility. Microdialysis measurement of acetylcholine levels shows higher ACh during movement than during immobility (Marrosu et al., 1995). Recording of GABAergic cells in the hippocampus and medial septum shows rhythmic firing during movement and less regular firing during immobility (Brazhnik & Fox, 1999; Fox et al., 1986). Both of these changes contribute to the appearance of theta rhythm oscillations in the hippocampal EEG during movement. (B) The theoretical mechanism of theta rhythm generation in the hippocampus. High levels of acetylcholine depolarize pyramidal cells and interneurons, causing them to generate spikes. Rhythmic GABAergic input to GABAergic interneurons in the hippocampus causes rhythmic changes in interneuron spiking activity, and rhythmic changes in pyramidal cell activity (Stewart & Fox, 1990). These effects in hippocampus and entorhinal cortex cause rhythmic changes in the strength of excitatory synaptic input to region CA1 from region CA3 and entorhinal cortex.

effects in the presence of acetylcholine, but the activation of feedback synapses in the presence of acetylcholine causes LTP which makes them stronger at later times. This paradoxical combination of effects can be understood in the context of associative memory models of piriform cortex and hippocampus (Hasselmo & Bower, 1993; Hasselmo & Schnell, 1994). Effective associative memory function requires that network activity be clamped to feedforward input during encoding, this prevents new associations from being distorted by the spread of activity across previously modified feedback connections. In contrast, during retrieval, activity must spread more freely across feedback synapses.

Thus, acetylcholine may prevent interference during the strengthening of feedback synapses by selectively suppressing excitatory feedback synapses but not feedforward synapses (Hasselmo, 1999; Hasselmo & Bower, 1993; Hasselmo & Schnell, 1994). At the same time, acetylcholine further enhances the response to feedforward input by causing post-synaptic depolarization of neurons (Barkai and Hasselmo, 1994; Benardo & Prince, 1982), suppression of neuronal adaptation (Barkai & Hasselmo, 1994) and suppression of feedback inhibition (Patil & Hasselmo, 1999). Modeling demonstrates that these combined physiological effects enhance encoding of new input patterns. This modeling is consistent with a general role for acetylcholine in setting the learning rate of cortical structures (see Doya, 1999, 2002). The level of cholinergic modulation can be regulated by the match of input with prior learning (Hasselmo & Schnell, 1994) causing effects relevant to the stable maintenance of prior associations (Carpenter & Grossberg, 1993). The regulation of relative strength of feedback connections is consistent with cholinergic regulation of top–down versus bottom–up influences on cortical representations (Yu & Dayan, 2002).

The role of acetylcholine in preventing interference during encoding has been supported by experimental work. Blockade of muscarinic acetylcholine receptors increases proactive interference from previous learning (DeRosa and Hasselmo, 2000; DeRosa, Hasselmo, & Baxter, 2001), and increases generalization between similar odorants (Linster & Hasselmo, 2001; Linster, Garcia, Hasselmo, Baxter, 2001). In addition, lesions of the fornix and medial septum, which remove cholinergic innervation of the hippocampus, cause impairments in tasks requiring learning of new responses to replace previously learned responses.

1.2. Theta rhythm may allow rapid transitions between encoding and retrieval

While it is important to prevent interference during encoding, it is important to have an ongoing ability to access hippocampal representations for retrieval. The relatively slow time course of muscarinic cholinergic effects on synaptic transmission and postsynaptic depolarization suggest that acetylcholine would require several seconds to change network dynamics (Hasselmo & Fehlau, 2001). This motivated a search for potential mechanisms allowing faster transitions between encoding and retrieval. Recent work suggests that rapid transitions between encoding and retrieval could be provided by theta rhythm oscillations (Hasselmo, Bodelon, & Wyble, 2002a), which are induced in the hippocampal formation due to rhythmic input to the hippocampus from both cholinergic and GABAergic cells of the medial septum (as summarized in Fig. 1B). Here we show how theta rhythm oscillations may provide a mechanism by which encoding and retrieval dynamics could rapidly alternate within the hippocampal formation, allowing encoding of new information without interference due to retrieval of previously encoded information.

During movement through the environment, the hippocampal EEG shows a prominent oscillation in the 6–12 Hz frequency range referred to as theta rhythm (Buzsaki, Leung, & Vanderwolf, 1983). This theta rhythm activity appears to be regulated by cholinergic and GABAergic input from the medial septum (Stewart & Fox, 1990), as shown in Fig. 1B. During theta rhythm, acetylcholine depolarizes both excitatory and inhibitory neurons in the hippocampus, and rhythmic GABAergic input to hippocampal interneurons causes rhythmic inhibition and

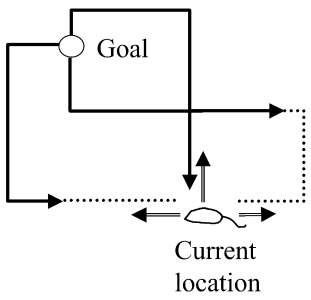

Fig. 2. Proposed mechanism for spatial navigation, allowing selection of the Shortest Path from the current location to the goal location. Activity spreads backward from the goal location A_g toward the current location along multiple different encoded pathways in $W_B = W_{ECIII}$ (shown by solid lines). When activity along the shortest pathway reaches the current location A_c, activity spreads forward one step from the current location along encoded pathways in $W_F = W_{CA3}$ (shown by double lines). As shown in the figure, these patterns of spreading activity will overlap first for the next step along the Shortest Path to the goal. The activity spreading along longer pathways has not yet reached the current location by the time the overlap occurs (dotted lines show portions of longer pathways not yet activated).

disinhibition during this slower cholinergic depolarization. Cutting the fornix destroys the cholinergic and GABAergic input from medial septum to the hippocampus, and causes a strong decrease in theta rhythm oscillations measured in the electroencephalograph (EEG) within the hippocampal formation (Buzsaki et al., 1983). Selective lesioning of the cholinergic input alone has been shown to greatly decrease the amplitude of theta rhythm oscillations (Lee et al., 1994). Selective lesions of the medial septum and portions of the fornix suggest that theta depends upon the afferent input from the medial septum, but not on the output pathways through lateral septum (Andersen, Bland, Myhrer, & Schwartzkroin, 1979; Rawlins, Feldon, & Gray, 1979).

The same manipulations which decrease theta rhythm amplitude also cause strong impairments on certain spatial navigation tasks. For example, cutting the fornix causes impairments in the ability of rats to perform certain tasks including spatial reversal in a T-maze (M'Harzi et al., 1987) and reversal in the Morris water maze (Whishaw & Tomie, 1997). Lesions of the medial septum also impair delayed alternation (Numan, Feloney, Pham, & Tieber, 1995).

Recently, a simplified mathematical analysis showed how loss of theta rhythm modulation could impair performance of spatial reversal in a T-maze task (Hasselmo et al., 2002a). Theta rhythm oscillations prove essential to effective spatial navigation function in integrate-and-fire simulations (Hasselmo, Cannon, & Koene, 2002b). The theta rhythm is associated with changes in synaptic currents and membrane potential in a number of different populations of neurons within subregions of the hippocampal formation, including region CA3, region CA1 and the entorhinal cortex (Bragin et al., 1995; Brankack, Stewart, & Fox, 1993; Stewart & Fox, 1990). Here we present hypotheses about the potential functional role of these theta rhythm oscillations in normal spatial navigation function.

2. Model of spatial navigation

2.1. Overview of technique

The analytical techniques presented here are used to link spatial navigation behavior to specific physiological variables in the hippocampal formation. These have been used previously in the specific example of reversal learning in the T-maze (Hasselmo et al., 2002a). The functional properties analyzed here have also been demonstrated in simulations using interacting populations of integrate-and-fire neurons to guide the movement of a virtual rat in a virtual environment (Hasselmo et al., 2002b). Here we provide a general overview of this technique, which should be applicable to a number of different instances.

Consider a rat foraging for food in an environment with a number of food sources in different locations. According to the model presented here, the hippocampal formation encodes memories of pathways that the rat traverses through the environment in search of food. Once multiple individual pathways have been stored, the navigational mechanism modeled here selects the shortest path to the closest food goal (cf. Muller & Stead, 1996). Throughout this paper we will refer to this pathway as simply the 'Shortest Path'. The Shortest Path is understood to be the path, which involves the smallest number of steps from any given location to the food source where the steps are taken along any one or combination of the stored paths. In other words, the rat combines known paths and segments of such paths to get to the closest food source in as few steps as possible. The basic mechanism is summarized in Fig. 2. The model incorporates physiological data to show how the hippocampus may operate to allow the rat to retrieve a memory of the Shortest Path. This is interesting because the memory may actually be a composite of earlier paths that have been traveled, rather than a memory of a single path that was actually traveled. Note that we focus specifically on the learning of multiple individual pathways, rather than the immediate activation of a two-dimensional map, as proposed in other work (Samsonovich & McNaughton, 1997). Both pathway based navigation and map-based navigation may coexist in the hippocampus. In fact, sufficient crisscrossing of an open environment on individual pathways will ultimately set up a two-dimensional representation of that environment (Blum & Abbott, 1993; Muller & Stead, 1996). In the open field or the Morris Water maze, visual inspection of the environment could allow rapid formation of a two-dimensional map, and rats clearly perform path integration to traverse previously untraversed pathways (Whishaw & Tomie, 1997). However, most wild rats spend much of their time in enclosed pathways which would favor pathway based navigation, and the fact that place cells are strongly dependent on direction of movement in tasks such as the 8-arm radial maze (McNaughton, Barnes, & O'Keefe, 1983) suggest there are distinct pathway based representations even for different directions in a single location. These

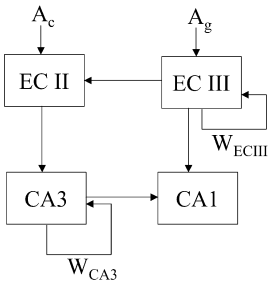

Fig. 3. Schematic representation of anatomical structures and connections used for spatial navigation in the model. Activity spreads backward from the goal location A_g across recurrent connections $W_{ECIII} = W_B$ in entorhinal cortex layer III (ECIII). This activity converges with afferent input representing current location A_c in entorhinal cortex layer II (ECII), causing spiking for current location when it matches the backward spread. This activity enters hippocampal region CA3, where activity spreads forward one step across recurrent connections $W_{CA3} = W_F$. The activities from region CA3 and from ECIII converge on region CA1. Region CA1 remains subthreshold except where the overlap of input from region CA3 and ECIII will cause spiking indicating the next step along the Shortest Path to the goal. Note that the model has been simplified by only assuming modification of recurrent connections in ECIII and in CA3. All other connections shown are represented in a simple manner by identity matrices, which directly transmit the pattern in one region to another region. The activity of this network is summarized in the following equations (Eq. (2.21) from text): $a_{ECIII} = W_B^M A_g = A_{g-M}$, $a_{ECII} = A_c$, $a_{CA3} = W_F a_{ECII} = W_F A_c = A_{c+1}$, $a_{CA1} = [a_{CA3} + a_{ECIII} - \mu]_+ = [W_F A_c + W_B^{M-1} A_g - \mu]_+$.

pathway specific representations may only become merged into non-directional map type representations after learning of associations between different path segments (Kali & Dayan, 2000).

The movement of the rat could be guided by a number of different mechanisms, corresponding to action selection in reinforcement learning (Sutton & Barto, 1998). In a general way, the action selection process in spatial navigation involves a selection of a next position on the basis of the current position and the goal location. In other words:

$$a_{k+1} = f[a_c, a_g] \tag{2.1}$$

where a_{k+1} represents the rat's next step as function of its current location a_c and current representation of the goal or food source location a_g.

Here we propose a specific mechanism for spatial navigation involving an interaction of subregions of the hippocampal formation. This mechanism will be described below.

The spatial navigation mechanism that we propose has a number of different dynamical variables. The relative timing of activity in these variables plays an important role in the ability of this mechanism to function in a stable and effective manner. Rather than turning these variables off and on in an algorithmic manner, we will allow them to vary in a continuous rhythmic manner analogous to the variation of specific physiological variables during theta rhythm. Section 3 will evaluate how the performance measure will change for different phase relationships of physiological variables using our specific mechanism of spatial navigation.

2.2. A specific proposed mechanism for spatial navigation

For selection of the next location, we propose an interaction of a number of different hippocampal subregions. The basic circuitry we have focused on is shown in Fig. 3, based on the anatomical circuits of the hippocampal formation (Amaral & Witter, 1989; Johnston & Amaral, 1998).

As shown in Fig. 3, the basic neural circuitry that is employed in the rat's navigational mechanism is organized in the following fashion: Activity in entorhinal cortex layer II is determined by afferent input from other neocortical structures as well as input from entorhinal cortex layer III. Activity in region CA3 is determined by input from entorhinal cortex layer II and from recurrent connections in region CA3. Activity in region CA1 is determined by input converging from CA3 and from entorhinal cortex layer III. Finally, activity in entorhinal cortex layer III is determined by input from the prefrontal cortex and from recurrent connections in entorhinal cortex layer III. We have not yet incorporated the function of the dentate gyrus into this computational simulation.

A full blown computational model of the neural circuits illustrated in Fig. 3 would need to include explicit equations for the strengthening of all the major sets of neural connections. This would include, at minimum, the connections between: (1) entorhinal cortex and region CA3, (2) region CA3 and region CA1, (3) region CA3 and itself, (4) entorhinal cortex layer III and itself, (5) entorhinal cortex layer III and region CA1, and (6) entorhinal cortex layer III and entorhinal cortex layer II (Johnston & Amaral, 1998). In Section 2, we assume that the connections (1, 2, 5 and 6) above are represented by an identity matrix, and we do not model them explicitly. We focus our attention on the recurrent connections (3) and (4) above in region CA3 and entorhinal cortex layer III, respectively. Later in Section 3, we will consider the implications of modifying connections (2) from region CA3 to region CA1.

As a simple overview, we propose that as the rat explores the environment, it learns a number of different pathways through its environment. This learning occurs during encoding phases which alternate with retrieval phases within each cycle of the theta rhythm. The pathways are encoded in two directions, forward and backward. It is proposed that the forward direction is encoded in the recurrent connections in regions CA3 and the backward direction in the recurrent connections of entorhinal cortex layer III.

We assume that these pathways are encoded via strengthening of synapses between place cells that correspond to specific locations in the environment. Place cells are individual rat hippocampal neurons which fire selectively when the rat is located in restricted spatial locations in

its environment (Mehta, Barnes, & McNaughton, 1997; Muller & Kubie, 1989; O'Keefe & Recce, 1993; Skaggs, McNaughton, Wilson, & Barnes, 1996). These cells have been characterized extensively in a variety of experiments, and often show firing strongly dependent upon the specific direction of movement which suggests specificity for specific pathways rather than general location (Markus et al., 1995; McNaughton et al., 1983; Skaggs et al., 1996). In fact, hippocampal neuronal responses may actually code individual events within any episode, whether it be spatial or non-spatial (Eichenbaum, Dudchenko, Wood, Shapiro, & Tanila, 1999). In the model presented here, active place cells correspond to a location in the environment and a sequence of activity of different place cells represents a path through the rat's environment. The paths may then be modeled as series of vectors of neural activation where each pattern of neuron activation in a particular stored sequence corresponds to a particular location. The correspondence between a pathway in the external environment and a particular sequence of vectors of neuron activation makes it possible to refer to the sequence of vectors of neuron activation as a 'pathway'. The word pathway is used below to refer to both geographic pathways and sequences of vectors of neuronal activation that correspond in a one-to-one fashion with geographic pathways. The context should make the meaning clear.

During navigation that takes place after initial exploration, the rat selects its movement by retrieving stored information on pathways. We propose that this retrieval occurs during specific phases of theta rhythm cycles, rapidly alternating with encoding phases during which the existing representation can be modified. The selection of movement along an individual pathway requires an interaction of neuron activity that spreads forward and backward through stored sequences of activity that correspond with a sequence of actual locations (i.e. a pathway) in the rat's environment. Specifically, we propose that activity spreads backward from cells representing the goal location along connections within entorhinal cortex layer III, and forward from cells corresponding to the current location along recurrent connections in region CA3. These two different directions of spread then converge in hippocampal region CA1. The convergence allows selection of the next step which, as we will show below, corresponds, under certain conditions, to the next step along the Shortest Path.

Our assumptions about backward and forward spread of activity and convergence of this activity in CA1 were motivated by and are consistent with some of the available experimental data on the hippocampal formation. This includes anatomical evidence for the strong recurrent connectivity in hippocampal region CA3 and the superficial layers of the entorhinal cortex (Amaral & Witter, 1989; Shepherd, 1998) and the largely unidirectional connectivity from these regions to region CA1. On a physiological level, the overall structure of the model was motivated by the difference in size of place fields in the hippocampus and entorhinal cortex (Barnes, McNaughton, Mizumori, Leonard, & Lin, 1990; Frank, Brown, & Wilson, 2001; Quirk, Muller, Kubie, & Ranck, 1992). Place fields are the spatial extent of the environmental locations in which a given neuron will fire. In particular, the place fields in region CA1 of the hippocampus are much smaller than place fields of cells in the deep layers of the entorhinal cortex, which is the dominant structure receiving output from region CA1 (Frank, Brown, & Wilson, 2000). This suggests that the tightly constrained spatial firing in the hippocampus is only used in regions CA3 and CA1. Here we assume that the constrained firing in region CA1 may be a representation of the next desired location of the rat, as supported by experimental evidence suggesting that place cells in region CA1 may predict the location of the rat in the next 120 ms (Muller & Kubie, 1989). At earlier and later stages the nature of the representation may differ. Here, we take the approach that the input regions of the entorhinal cortex show larger place fields due to spreading of activity between associated places, and the output layers of entorhinal cortex would start transforming next desired location into coordinates for the next movement. The broad spread of activity is consistent with the fact that entorhinal cortex lesions impair learning of simple associations, suggesting it is the locus for storage of simple inter-item associations, whereas the hippocampus is involved in more complex relational representations (Bunsey & Eichenbaum, 1993).

2.3. Review of integrate-and-fire simulation

The mechanism described here has been analyzed in a simulation incorporating populations of integrate-and-fire neurons representing multiple different regions (Hasselmo et al., 2002b). There is insufficient space to present details of this model here. However, a simple example from this model illustrates the basic mechanism for guiding navigation with the interaction of entorhinal cortex, regions CA3 and CA1. The spread of spiking activity in the integrate-and-fire model is shown in Fig. 4, for the simple behavior of a virtual rat in a virtual T-maze environment. The figure shows activity when the virtual rat is at the choice point of the maze, after it has already encoded associations between adjacent spatial locations in all portions of the maze. On the top, entorhinal cortex layer III receives input from the prefrontal cortex representing the food location in the left arm of the maze. Activity spreads backward from the food location to sequentially activate place cells representing the locations in the left arm, in the stem and in the right arm. When this activity reaches neurons representing the current location, it causes activity to start in region CA3 (bottom). The activity spreads forward one step in CA3, corresponding to spatial locations in all directions from the virtual rat

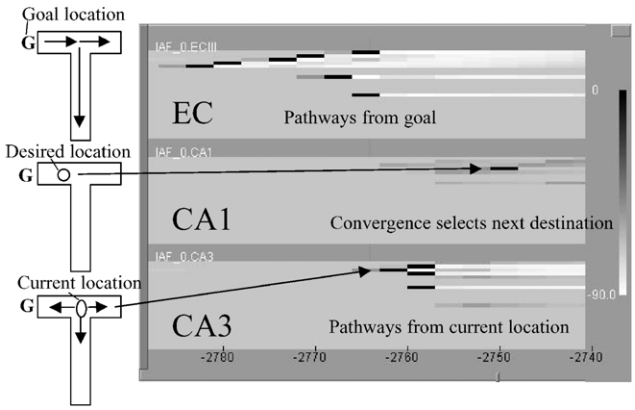

Fig. 4. Network activity during goal directed navigation. Each rectangle shows the activity within a specific simulated region, with time plotted horizontally and individual neurons plotted vertically. Individual spikes appear as black rectangles. On the left, a schematic of the T-maze shows how the activity of cells in the simulation corresponds to mental representations of the environment. In EC layer III (top), input from prefrontal cortex induces a spike at the goal location, and spiking spreads back from goal location through neurons representing adjacent locations into neurons representing the stem and right arm of the maze. When this activity reaches the current location, it causes spiking in EC layer II (not shown) which induces a spike in the place cell representing current location in CA3 (bottom). Spiking activity in CA3 spreads forward one step from current location before feedback inhibition shuts it off. The spiking activity in CA3 and EC layer III converges on region CA1, where it causes spiking in a neuron representing the next desired location. The virtual rat then moves to this next desired location. These mechanisms allow selection of the next step along the shortest pathway to the closest goal.

(into the left arm, right arm and stem). Convergent input from region CA3 and entorhinal cortex layer III causes a single spike in region CA1 representing the next desired location of movement toward the goal—in this case in the left arm of the T-maze. The virtual rat moves to this location, and the retrieval dynamics are repeated for the new current location.

2.4. Mathematical description

This section will provide a more detailed mathematical description of this theoretical mechanism.

The location of the rat in its environment is represented by a pattern of neuron activity corresponding to place cell responses in the hippocampal formation. We do not explicitly model the formation of place cell responses, but instead assume that place cell responses already exist. All the locations in the environment are numbered $1-n$. At each step, the location of the rat is modeled as an n-dimensional vector ('location vector') which has the binary elements 1,0. The rat's location in the environment is indicated by giving a value of 1 to the appropriate element of the location vector and a 0 to all other elements. For example, if the rat is at location number j, then the jth element of the location will have the value 1, and all other elements will have the value 0. Note that this is a discrete representation of space which simplifies analysis of the model. However, it does not address possible functional properties associated with the overlapping fields of place cells observed in physiological recording (Mehta et al., 1997; Skaggs et al., 1996).

Using this approach, a journey of the rat through the environment can be represented as a sequence of n-dimensional binary vectors. Each location in the rat's journey is represented by a single vector which has the appropriate element set to the value 1 and all other elements set to the value 0. The entire journey is a sequence of such vectors. A subscript is then introduced to indicate the relative position of a location vector within a sequence of vectors that represents a journey. For example, the sequence $\{a_i, a_{i+1}, \ldots, a_{i+k}\}$ represents the sequence of locations traversed by the rat from the i to $i+k$ steps on a particular journey through its environment. It should be emphasized that the subscript in this case refers only to the relative position of a location vector in a sequence of locations that constitute a particular journey. The indexes do not refer to locations in any absolute sense, i.e. independent from their meaning in a particular journey through the environment. For example, if a rat is at the same location on the ith and $(i+k)$th steps of the journey segment represented above, then it would follow that $a_i = a_{i+k}$—which is equivalent to stating that $\alpha_{ji} = \alpha_{jk}$ for all j, $j = 1 \ldots n$, where α_{ji}, α_{jk} are the jth elements of the locations vectors a_i, a_k, respectively. From a geographic point of view, the statement that $a_i = a_{i+k}$ means that the rat's path loops back upon itself in at least one location. We will use lower case letters in a subscript index, e.g. a_i, a_k when referring to vectors within a particular sequence. We will refer to the total number of locations traversed in a pathway with the upper case letter K. When we wish to refer to an absolute location, we will use upper case letters: e.g. A_g refers to the absolute location of some goal g, independent of any particular sequence of locations leading to this goal.

In addition to location vectors which show the rat's location on a particular journey, we will also make use of location vectors that represent retrieved information about the location of the rat along particular journeys during certain phases of theta rhythm. These are the same n-dimensional vectors. The only difference is that when the rat is retrieving information about past locations in multiple journeys that vectors of retrieved location information may have more than a single element set to the value 1. This is shown in more detail below.

A location vector, a, is a column vector. Its transpose a^{T} is a row vector. The expression $a_i^{\mathrm{T}} a_k$ is the inner product that is obtained as follows:

$$a_i^{\mathrm{T}} a_k = \sum_{j=1}^{n} \alpha_{ji} \alpha_{jk} \tag{2.2}$$

where α_{ji}, α_{jk} are the jth elements of the locations vectors

a_i, a_k, respectively. Obviously Eq. (2.2) is a scalar value. Note that if we take the inner product of location vectors from a particular journey, then it is the case that:

$$a_i^{\mathrm{T}} a_k = \begin{cases} 1 & \text{if } a_i = a_k \\ 0 & \text{if } a_i \neq a_k \end{cases} \tag{2.3}$$

The expression $a_i a_k^{\mathrm{T}}$ is the outer product of the vectors a_i, a_k which is the matrix:

$$a_i a_k^{\mathrm{T}} = \begin{matrix} \alpha_{1i}\alpha_{1k} & \alpha_{1i}\alpha_{2k} & \cdots & \alpha_{1i}\alpha_{nk} \\ \alpha_{2i}\alpha_{1k} & \alpha_{2i}\alpha_{2k} & \cdots & \alpha_{2i}\alpha_{nk} \\ \vdots & & & \\ \alpha_{ni}\alpha_{1k} & \alpha_{ni}\alpha_{2k} & \cdots & \alpha_{ni}\alpha_{nk} \end{matrix} \tag{2.4}$$

where α_{ji}, α_{jk} are the jth elements of the locations vectors a_i, a_k, respectively.

We will also frequently make use of the following associative property that results when we pre-multiply a vector by an outer product matrix:

$$\left(a_i a_k^{\mathrm{T}}\right) a_j = a_i \left(a_k^{\mathrm{T}} a_j\right) \tag{2.5}$$

This identity clearly holds equally well if we pre-multiply a vector by a sum of outer product matrices, e.g.

$$\left(\sum_{k=1}^{K} a_{k-1} a_k^{\mathrm{T}}\right) a_j = \sum_{k=1}^{K} a_{k-1} \left(a_k^{\mathrm{T}} a_j\right) \tag{2.6}$$

Entorhinal cortex layer III and region CA3 are distinguished by the high level of recurrent connectivity in these regions. We assume that the connectivity in these regions is established during learning that takes place as a result of the sequential activation of place cell representations which are modeled here as location vectors. This occurs during specific encoding phases of the theta rhythm oscillations. The place cell representations (location vectors) are activated in sequence as the rat moves through its environment. As modeled explicitly below, during an encoding phase, this sequence of activity creates and strengthens connectivity between neurons within entorhinal cortex layer III as well as within region CA3 so that locations that are next to each other in a particular journey are retrieved as a sequence during recall (cf. Levy, 1996). The modified synaptic connections are represented by outer products of the location vectors. Initially, we will assume that the creation of recurrent synaptic connectivity in entorhinal cortex layer III and region CA3 occurs in an encoding phase within each theta rhythm cycle, during which there is no spread of activity across synaptic connections, rapidly alternating with a retrieval phase during which activity can spread across synaptic connections. Later, when we discuss the function of theta rhythm, we will analyze the functional effects of oscillatory modulation of spread of activity across synaptic connections in region CA3.

For reasons that will become evident below, we define the learning of forward connections in region CA3 and the backward connections in entorhinal cortex layer III. Here the terms forward and backward refer to the order of a sequence of locations through an environment as they were traversed by the rat. Forward connections are those that are formed based on ordering the sequence of location vectors in the same order that the rat traveled the locations in the actual journey. Backward connections are those that are formed when the sequence of locations vectors that represent a journey is reversed so that the first location is last, the second location is second to last, etc. With this terminology in mind, the forward connections in region CA3 and the backward connections in entorhinal cortex layer III are modeled with two matrices $W_{\mathrm{F}}, W_{\mathrm{B}}$, respectively. The two matrices $W_{\mathrm{F}}, W_{\mathrm{B}}$ are obtained as follows:

$$W_{\mathrm{F}} = \sum_{k=1}^{K} a_{k+1} \cdot a_k^{\mathrm{T}} \tag{2.7}$$

$$W_{\mathrm{B}} = \sum_{k=1}^{K} a_{k-1} \cdot a_k^{\mathrm{T}} \tag{2.8}$$

where lower case k is the index of positions in a pathway, and upper case K is the total number of positions traversed. The matrices $W_{\mathrm{F}}, W_{\mathrm{B}}$ give in explicit form the set of connections that have formed in CA3 and entorhinal cortex layer III as the result of a particular journey by the rat through the environment. Note that we assume Hebbian synaptic modification with presynaptic activity preceding postsynaptic depolarization in both cases (Levy & Steward, 1983). The different direction of connectivity can be obtained with a buffering of activity due to calcium-sensitive cation currents (Fransen, Alonso, & Hasselmo, 2002; Jensen & Lisman, 1996), which can buffer information in different sequential orders. For example, in response to a sequence of input patterns A–B–C, these mechanisms can repetitively replay ABC or CBA, allowing encoding with different directionality.

How is information retrieved once it has been encoded in the matrices $W_{\mathrm{F}}, W_{\mathrm{B}}$? We now show the mathematical basis on which useful information can be retrieved from the recurrent connections that formed during encoding and that are modeled in the matrices $W_{\mathrm{F}}, W_{\mathrm{B}}$. We assume that after learning how to get to certain goals, the rat is able to retrieve information which can guide the rat from its current location, A_c, to some goal location, A_g, where the rat has previously found food sources. Detailed simulations have focused on the mechanisms for establishing goal representations in prefrontal cortex and providing this goal input during retrieval, but here we simply assume that the goal representation process selectively gives input, which causes the activity in entorhinal cortex layer III to reflect goal locations $a_{\mathrm{ECIII}} = A_g$, and as discussed below, the spread of activity along known paths from the goal locations.

Note that we use the notation $a_{\mathrm{CA3}}, a_{\mathrm{ECIII}}, a_{\mathrm{ECII}}, a_{\mathrm{CA1}}$ to

indicate the activity of neurons in the regions CA3, ECIII, ECII and CA1, respectively. For the sake of simplicity, we assume that the dimensionality of the activity vectors in each of these regions is identical, i.e. activity in each region can be represented by an n-dimensional vector, and the connectivity matrices are all square $n \times n$ matrices. The lower case letters used to show activity in a region should not be confused with those used to show location vectors in a sequence—each region could have many different location vectors.

In order to show how information is retrieved, we assume that encoding has taken place (during encoding phases of theta) and that the matrix W_B of connectivity has been created according to Eq. (2.8). In this case, during the retrieval phase of each theta cycle, the vector of activity in ECIII, $a_{ECIII} = A_g$, will spread backwards through the sequence of place cell representations that were active when the rat traveled to the goal location. The combined impact on ECIII activity of the active goal location vector, A_g and recurrent ECIII connections is shown by pre-multiplying A_g by the matrix W_B to obtain:

$$W_B A_g = \left(\sum_{k=1}^{K} a_{k-1} a_k^T \right) A_g \tag{2.9}$$

We determine the subsequent step of activity by evaluating Eq. (2.9) which can be done by taking advantage of the properties of the inner product in Eq. (2.3) so that:

$$a_k^T A_g = \begin{cases} 1 & \text{if } a_k = A_g \\ 0 & \text{if } a_k \neq A_g \end{cases} \tag{2.10}$$

We may the evaluate Eq. (2.9) as:

$$W_B A_g = \left(\sum_{k=1}^{K} a_{k-1} a_k^T \right) A_g = \sum_{k=1}^{K} a_{k-1} \left(a_k^T A_g \right) \tag{2.11}$$

But according to Eq. (2.10) the inner product in Eq. (2.11) is equal to 0 everywhere except where the vector $a_k = A_g$ and in this case the inner product is equal to 1. It is then easy to see that the only vector from the sum of vectors $\sum_{k=1}^{K} a_{k-1}$, which survives post-multiplication by the inner product $(a_k^T A_g)$, is the vector a_{g-1}. This is because where $a_k = A_g$, the vector a_{k-1} survives (it is multiplied by 1 instead of 0 for all other vectors), but $a_{k-1} = a_{g-1}$. We use the smaller case in a_{g-1} to indicate that the vector is the location vector a_{g-1} from the specific sequence $\{a_i\}$. In the sequence $\{a_i\}$ the location vector a_{g-1} is the vector, which is one step in the sequence away (in the backward direction) from the goal location.

The reasoning above gives the final result for ECIII activity after one step of spread from the goal location as:

$$a_{ECIII} = W_B A_g = \sum_{k=1}^{m} a_{k-1} a_k^T A_g = a_{g-1} \tag{2.12}$$

where $a_{g-1} \in \{a_i\}$ where $\{a_i\}$ is the training sequence which was used to form the matrix W_B according to Eq. (2.8). Eq. (2.12) assumes that a single path to the goal has been stored and that this path, at least at the point, A_g, does not intersect or loop back on itself. In the case, where the path loops back on itself at point A_g, it would be necessary to modify Eq. (2.12) to show that the backward flow of activity can generate the activity of multiple place cells representing the backward flow of activity along the loop and cutting out the loop. This issue is discussed in more detail below.

It then follows through repetitive application of the result from Eq. (2.12) that activity will continue to spread along recurrent connections, so that after M cycles of spreading activity, activity in ECIII will take the value:

$$a_{ECIII} = W_B \cdots W_B W_B A_g = W_B^M A_g = a_{g-M} \tag{2.13}$$

where a_{g-M} represents the location which is M steps prior to the food source location A_g in the sequence $\{a_i\}$. Again we note that Eq. (2.13) assumes a single path, which does not loop back upon or intersect with itself.

We use the following equation for activity in entorhinal cortex layer II:

$$a_{ECII} = A_c \tag{2.14}$$

As Eq. (2.14) suggests we assume that entorhinal cortex layer II represents the rat's current location. Our assumption that activity of entorhinal cortex layer II is limited to the current location should be understood as only an approximation of the input from entorhinal cortex layer II to region CA3. Although experimental data suggests that entorhinal cortex has wider place fields, we believe that Eq. (2.14) gives a useful approximation of the role that entorhinal cortex layer II activity plays relative to region CA3 in rat navigation. The wide place field provided for in Eq. (2.13) is more consistent with experimental data regarding the size of place fields in the entorhinal cortex (Barnes et al., 1990; Frank et al., 2000; Quirk et al., 1992).

The representation of current location becomes activated at the time that the backward spread of activity in entorhinal cortex layer III reaches current location. In simulations (Hasselmo et al., 2002b), this ensures the correct timing of convergence in region CA1 as described below. When current location activity is initiated in entorhinal cortex layer II, this then causes activity in region CA3 to match current location ($a_{CA3} = A_c$) and then to spread forward a short distance (just one step in this example).

$$a_{CA3} = W_F A_c = \sum_{k=1}^{K} a_{k+1} a_k^T A_c = A_{c+1} \tag{2.15}$$

We assume that the spread of activity in region CA3 is more limited than the spread of activity in the entorhinal cortex - as represented above in Eq. (2.13). The much smaller spread in region CA3 relative to entorhinal cortex satisfies an important physiological constraint—place cells in region CA3 and CA1 have much smaller place fields than those observed in entorhinal cortex (Barnes et al., 1990; Frank et al., 2000; Quirk et al., 1992). This difference in relative

size of place fields is obtained in our model by restricting the spread of activity in region CA3, while allowing much broader spreading of activity in entorhinal cortex layer III. The much smaller spread in region CA3 also may have an important functional role. If our model is correct, then a greater spread of activity in region CA3 can actually worsen performance of the rat's navigation mechanism by causing selection of incorrect destination activity.

The selection of the next step toward the goal location is obtained through a convergence of the backward spread with the forward spread in region CA1. Activity in CA1 results from interactions of the backward spread from entorhinal cortex layer III arriving via the perforant path and the forward spread in hippocampal region CA3 arriving via the Schaffer collaterals. We assume that the resulting activity in CA1 represents or predicts the next step that the rat will make in its environment. Experimental data is broadly consistent with our model's assumptions regarding the role of CA1 in representing the rat's next step. Research suggests that place cells might fire just in advance of the movement of a rat into the place field of the cell (Muller & Kubie, 1989). The phenomenon of theta phase precession (O'Keefe and Recce, 1993; Skaggs et al., 1996) can also be interpreted this way. As a rat first moves into the place field of a place cell in region CA1, spiking activity occurs late in the theta cycle (during the retrieval phase), whereas spiking activity appears earlier in the theta cycle (during the encoding phase) as the rat moves into the field. This is consistent with the notion that predictive activity may be selective to one cycle of the theta oscillation, as appears when we consider theta function below.

The role we have proposed for region CA1 in representing the rat's next step has natural consequences for the measure of the performance of the navigational mechanism. The proposed navigational mechanism will achieve high performance only if the activity in region CA1 during the retrieval phase accurately represents or predicts the next step from the current location along the shortest path to the closest food source location. Deviations or malfunctions of CA1 in this regard should result in reduced performance.

In order for convergence of forward and backward activity in CA1 to lead to high navigational performance, it is important that the forward and backward activity be matched in their timing in a certain way. This result is achieved in our model by assuming that the forward and backward activities arrive in phase in region CA1. However, we propose further that the convergence of similarly timed forward activity and backward activity will not generate activity in CA1 unless the two inputs represent the same absolute location. In other words, we assume that separate arrival of an element of backward or forward activity in region CA1 results in subthreshold activity. Only if forward and backward activity matches does the sum of this converging activity cause the binary 'spiking' activity in CA1.

To make the advantages of this approach clearer, we may consider the case where the current location is part of a sequence of locations that includes the food source location (i.e. $A_c, A_g \in \{A_i\}$). Backward activity from entorhinal cortex layer III continues to spread but does not generate activity in region CA1 until the backward activity matches the converging activity from CA3. In other words no activity in CA1 is generated until:

$$a_{CA3} = W_F A_c = A_{c+1} = a_{ECIII} = W_B^{M-1} A_g = A_{g-M+1} \tag{2.16}$$

where M represents the number of steps along the shortest path between the current location and that food location. When condition (2.16) is satisfied, CA1 activity occurs and represents, as we prove below, the Shortest Path.

The assumption that separate inputs from CA3 and entorhinal cortex layer III are subthreshold on their own is necessary to ensure that CA1 will only become active when it represents the next step along the shortest path. This can only take place when the inputs to CA1 from CA3 and entorhinal cortex layer III match in CA1. We represent our assumptions that: (a) the individual inputs to CA1 from entorhinal cortex layer II and CA3 are subthreshold and (b) the sum of matching inputs exceeds activation threshold in CA1 with the following notation:

$$a_{CA1} = [a_{CA3} + a_{ECIII} - \mu] + = \left[W_F A_c + W_B^{M-1} A_g - \mu \right]_+ \tag{2.17}$$

The notation $[\ ]_+$ indicates that the ith element of a_{CA1} will be active if: $(a_{CA3})_i + (a_{ECIII})_i > \mu$ where $(a_{CA3})_i, (a_{ECIII})_i$ represent the ith elements of the vectors a_{CA3}, a_{ECIII}, respectively, and μ is the threshold, and where it is assumed that the individual inputs $(a_{ECIII})_i < \mu$ and $(a_{CA3})_i < \mu$.

2.5. Problem of 'Skip Ahead'

One of the questions that immediately arises from Eq. (2.17) is: If signals from CA3 and entorhinal cortex layer III are constantly arriving in CA1, what prevents convergence of input at some location other than the current location plus one step. If CA3 activity continues to spread forward from the current location, beyond the single step proposed in Eq. (2.17) and entorhinal cortex layer III activity spreads backward from the goal location, it is possible for there to be convergence of these two inputs in CA1 at some location that is relatively far from the current location. In other words, if the spread of CA3 cannot be contained it might be the case that the relevant equation for CA1 activity becomes:

$$a_{CA1} = \left[W_F^K A_c + W_B^{M-K} A_g - \mu \right]_+, \qquad K \gg 1 \tag{2.18}$$

The outcome described in Eq. (2.18) might disrupt the rat's ability to navigate since it would be recalling locations far from the current location without recalling

the steps in between. It would be as if on the way to work one could remember an intersection that is halfway between work and home, but one could not remember how to get to the intersection. We call the problem illustrated in Eq. (2.18) the skip ahead problem. This skip ahead can be partly prevented by allowing only one step of activity spread along forward connections, but another form of skip ahead can result from the spread of CA3 retrieval activity during encoding. This issue has been extensively discussed in another context (Hasselmo et al., 2002a). This may easily interfere with the process of encoding new information. We can model the problem mathematically by considering the encoding Eq. (2.7) again. In the case where activity in region CA3 spreads during encoding the equation might look like:

$$W_{\mathrm{CA3}} = \sum_{k=1}^{K} \left(a_{k+1} + W^{i}_{\mathrm{CA3}} a_k\right) a_k^{\mathrm{T}} \tag{2.19}$$

where $W^{i}_{\mathrm{CA3}} a_k$ is a term which represents spread from the kth location during the encoding phase i steps forward. This would occur due to spread across previously modified recurrent connections in region CA3. This term might also be some more complicated combination of spreading of current and past activities. In either case, the spreading term in Eq. (2.19) would also be encoded and then retrieved during the retrieval phase. In other words:

$$a_{\mathrm{CA3}} = W_{\mathrm{F}} A_{\mathrm{c}} = \sum_{k=1}^{K} \left(a_{k+1} + W^{i}_{\mathrm{CA3}} a_k\right) a_k^{\mathrm{T}} A_{\mathrm{c}} = A_{\mathrm{c}+1} + W^{i}_{\mathrm{CA3}} A_{\mathrm{c}} \tag{2.20}$$

This spreading term could converge in CA1 with input from entorhinal cortex layer III to generate erroneous predictions. The retrieval of the spreading term could also cause skip ahead and prevent the hippocampal navigational mechanisms from generating the next step along the Shortest Path.

2.6. Problem of 'No Next Step'

Another problem might result if the activity generated in CA3 by input from entorhinal cortex layer II were to converge in CA1 with input from entorhinal cortex layer III, before forward spreading in CA3. This might happen if the backward spread of activity from entorhinal cortex layer III were to already be at the current location when CA3 first spikes in response to input from entorhinal cortex layer II at a new location. In this case, the rat might think its current location is the next step. We call this problem the No Next Step problem because CA1 does not generate a true next step—but simply continues to fire at the current location.

In order for the navigational mechanism described in this paper to perform well, there must be some mechanism in place in the hippocampal formation that ensures convergence of inputs in CA1 according to Eq. (2.16). We propose below that phase relationships in neuronal activity in the hippocampal formation may be important in ensuring the proper convergence of inputs in CA1 to generate the next step along the Shortest Path. As we show below, the phase relationships are important to minimize the Skip-Ahead and No Next Step problems.

2.7. In absence of activity during retrieval phase, exploration is assumed

Another important case concerns the situation when the current location is not part of any sequence of stored locations that leads to a food goal. In this case, there would be no matching input from region CA3 and entorhinal cortex layer III and, consequently, no activity in CA1. In this case, the rat must engage in exploration and cannot be limited to the exploitation of known paths to the food source, which provide no link with the current location. In this case, we assume that the rat's next step is generated in some probabilistic way in some other part of the brain. If movement takes place along learned pathways, then region CA1 may generate output which inhibits the exploratory movements and causes the rat to move along one of the learned pathways.

These types of issues have been addressed in reinforcement learning (Doya, 1999; Sutton & Barto, 1998), but are not addressed here explicitly.

When the rat engages in exploration, each step along the new exploratory pathway would be used during the encoding phase to update the recurrent connections in region CA3 as formalized in Eq. (2.7). When the rat moves to a new location, afferent signals to entorhinal cortex layer II generate a new current location representation which spreads through region CA3 and entorhinal cortex layer III and again converges in CA1. This activity either generates a next step based on known paths, as described above, or sends signals to other parts of the brain to generate an exploratory response.

In summary, we have four equations representing the activity patterns in the four subregions shown in Fig. 3:

$$\begin{aligned} a_{\mathrm{ECIII}} &= W_{\mathrm{B}}^{M} A_g = A_{g-M}, \qquad a_{\mathrm{ECII}} = A_{\mathrm{c}}, \\ a_{\mathrm{CA3}} &= W_{\mathrm{F}} a_{\mathrm{ECII}} = W_{\mathrm{F}} A_{\mathrm{c}} = A_{\mathrm{c}+1}, \\ a_{\mathrm{CA1}} &= [a_{\mathrm{CA3}} + a_{\mathrm{ECIII}} - \mu]_{+} = \left[W_{\mathrm{F}} A_{\mathrm{c}} + W_{\mathrm{B}}^{M-1} A_g - \mu\right]_{+} \end{aligned} \tag{2.21}$$

To provide a more complete picture of the navigational mechanism, we need to take into account the fact that the recurrent connections in region CA3 and entorhinal cortex layer III need to be able to store sequences of neuron activity that correspond to multiple pathways through the rat's environment to a given goal. To justify the particular navigational mechanism presented in this paper, it is also necessary to show that this mechanism will select the

shortest path among a collection of known pathways to a given goal.

2.8. Storage of multiple pathways

As a first step to the consideration of multiple pathways, Eqs. (2.7) and (2.8) should be modified to indicate that the recurrent connections are modified along each pathway that arrives at a given goal. The index P below is used to indicate each unique path that the rat has traveled over a given time period to a given goal location. This may be represented formally as:

$$W_{\mathrm{F}} = \sum_{j=1}^{P} \sum_{k=1}^{K} a_{k+1}^{j} a_{k}^{j\mathrm{T}} \tag{2.22}$$

$$W_{\mathrm{B}} = \sum_{j=1}^{P} \sum_{k=1}^{K} a_{k-1}^{j} a_{k}^{j\mathrm{T}} \tag{2.23}$$

It then must be noted that when activity spreads backward from a goal location in entorhinal cortex layer III, this spread results in a vector of neuronal activity at each step, which shows all of the locations that are within a certain number of steps of the goal location. This is represented formally as follows:

$$W_{\mathrm{B}} A_g = \sum_{j=1}^{P} \sum_{k=1}^{K} a_{k-1}^{j} a_{k}^{j\mathrm{T}} a_g = \sum_{j=1}^{P} \sum_{k=1}^{K} a_{g-1}^{j} \delta_{k,g}^{j}, \tag{2.24}$$

where $\delta_{k,g}^{j} = \begin{cases} 1 & a_k^j = a_g \\ 0 & a_k^j \neq a_g \end{cases}$

where a_{g-1}^{j} is a vector which corresponds to each of the locations that is located one iteration of activity spread away from the goal location. Note that the multiple path operator in Eq. (2.24) can output locations that are more than a single step back along the path. This is because paths may loop back on themselves and intersect with other paths. Thus activity spreading backward from a certain location $a_k = a_g$ will spread along all trajectories that lead to a_g. When a path loops back on itself at a_g after r steps (e.g. $a_k = a_g = a_{k+r}$), the operator in Eq. (2.24), will output the locations a_{k-1}, a_{k+r-1}. This effect is modeled with the use of the kronecker delta, $\delta_{k,g}^{j}$, in Eq. (2.24). As indicated in Eq. (2.24) that operator will output all locations that are $k-1$ steps from the current location along any path so long as there is an intersection between the kth step along the path and goal location. This takes into account intersections. For example, suppose that activity is spreading in the reverse direction along path s_1 and that the spread of activity reaches an intersection between paths s_1 and s_2. Given the existence of the intersection, it will be the case that $\delta_{k_{s1},k_{s1}} = \delta_{k_{s1},k_{s2}} = 1$ because $a_{k_{s1}} = a_{k_{s2}}$. This implies that the activity will spread, in the operators' next iteration, along both paths s_1 and s_2.

Similarly the continued spread of activity in entorhinal cortex layer III for two steps will result in a vector of activity that contains all locations that can be reached within two iterations of the operator in Eq. (2.24). With a change of index ($j \rightarrow s_1$), we may express the result of two iterations of the W_{B} operator as:

$$W_{\mathrm{B}}^{2} A_g = W_{\mathrm{B}}(W_{\mathrm{B}} A_g) = \sum_{j=1}^{P} \sum_{k=1}^{K} a_{k-1}^{j} a_{k}^{j\mathrm{T}} \left(\sum_{s_1=1}^{P} \sum_{k_{s_1}}^{K} a_{k_{s_1}-1}^{s_1} \delta_{k_{s_1},g}^{s_1} \right) \tag{2.25}$$

We may then change the order of summation in Eq. (2.25) to obtain:

$$W_{\mathrm{B}}^{2} A_g = \sum_{s_1=1}^{P} \sum_{k_{s_1}=1}^{K} \left(\sum_{s_2=1}^{P} \sum_{k_{s_2}=1}^{K} a_{k_{s_2}-1}^{s_2} a_{k_{s_2}}^{s_2 T} \right) a_{k_{s_1}-1}^{s_1} \delta_{k_{s_1},g}^{s_1} \tag{2.26}$$

and finally:

$$W_{\mathrm{B}}^{2} A_g = \sum_{s_1,s_2}^{P} \sum_{k_{s_1},k_{s_2}}^{K} a_{k_{s_2}-1}^{s_2} \delta_{k_{s_2},k_{s_1-1}}^{s_2,s_1} \delta_{k_{s_1},g}^{s_1} \tag{2.27}$$

Eq. (2.27) shows that two steps of activity spread in entorhinal cortex layer III result in active locations along paths that intersect with paths that intersect with the goal location.

Similarly if activity spreads through n steps, the result will be:

$$W_{\mathrm{B}}^{N} A_g == \sum_{s_1,s_2,\ldots,s_n}^{P} \sum_{k_{s_1},k_{s_2},\ldots,k_{s_n}}^{K} a_{k_{s_n}-1}^{s_n} \delta_{k_{s_n},k_{s_{n-1}}-1}^{s_n s_{n-1}}, \ldots, \delta_{k_{s_2},k_{s_1}-1}^{s_2,s_1} \delta_{k_{s_1},g}^{s_1} \tag{2.28}$$

or to simplify notation, we may write:

$$W_{\mathrm{B}}^{N} A_g = \sum_{s_1,\ldots,s_n,k_{s_1},\ldots,k_{s_n}}^{P,K} a_{k_{s_n}-1}^{s_n} \prod_{i=2}^{n} \delta_{k_{s_i},k_{s_{i-1}}-1}^{s_i s_{i-1}} \delta_{k_{s_1},g}^{s_1} \tag{2.29}$$

which again shows that after n steps of activity spread, locations will be active that are along paths that intersect with paths, that intersect with paths…that intersect with the goal location.

In the notation in Eq. (2.28) the separate indices $s_1, s_2, \ldots, s_n$ are needed to indicate the pathways along which activity has spread to reach a particular location. For instance, the notation $\delta_{k_{s_n},k_{s_{n-1}}-1}^{s_n s_{n-1}} \delta_{k_{s_1},g}^{s_1}$ indicates a specialized kronecker delta that will take the value 1 if it is possible to string together n unbroken path segments to reach the location $a_{k_{s_n}}$, otherwise the kronecker delta takes the value 0. Each segment may be taken from any path, so long as the resulting path is unbroken. This retrieval mechanism will quickly locate short cuts, and, as we show below, find the Shortest Path.

What happens in region CA1 when we take into account the possibility of multiple intersecting paths and loops? We recall from Eq. (2.17) that activity in region CA1 only results when matching inputs converge from CA3 and entorhinal cortex layer III. In Eq. (2.29) we

have proposed how activity will spread in entorhinal cortex layer III in the multiple path case. We may apply the same logic to obtain the forward spread of activity in CA3 as:

$$W_{\mathrm{F}}A_{\mathrm{c}} = \sum_{j=1}^{P}\sum_{k=1}^{K} a_{k+1}^{j}a_{k}^{j}a_{\mathrm{c}} = \sum_{j=1}^{P}\sum_{k=1}^{K} a_{k+1}^{j}\delta_{k,c}^{j} \tag{2.30}$$

$$\text{where } \delta_{k,c}^{j} = \begin{cases} 1 & a_{k}^{j} = a_{\mathrm{c}} \\ 0 & a_{k}^{j} \neq a_{\mathrm{c}} \end{cases}$$

Eq. (2.17) may then be rewritten in the multiple path case as:

$$\begin{aligned} a_{\mathrm{CA1}} &= \left[a_{\mathrm{CA3}} + a_{\mathrm{ECIII}} - \mu \right]_{+} \\ &= \left[W_{\mathrm{F}}A_{\mathrm{c}} + W_{\mathrm{B}}^{M-1}A_{g} - \mu \right]_{+} = \left[\sum_{j=1}^{P}\sum_{k=1}^{K} a_{k+1}^{j}\delta_{k,c}^{j} \right. \\ &\quad \left. + \sum_{s_{1,\ldots,m-1},k_{1,\ldots,m-1}}^{P,K} a_{k_{s_{m-1}}-1}^{s_{m-1}} \prod_{i=2}^{m-1} \delta_{k_{s_i},k_{s_{i-1}}-1}^{s_i s_{i-1}} \delta_{k_{s_1},g}^{s_1} - \mu \right]_{+} \end{aligned} \tag{2.31}$$

Note that as in the case of Eq. (2.17), where the one step of forward activity through region CA3 matches the $M-1$ cycles of backward activity through entorhinal cortex layer III the combined inputs are above threshold and cause spiking in region CA1.

One of the most important conclusions that emerges from the above analysis is that where $W_{\mathrm{F}}A_{\mathrm{c}} + W_{\mathrm{B}}^{M-1}A_{g} > \mu$, then $W_{\mathrm{F}}A_{\mathrm{c}} = W_{\mathrm{B}}^{M-1}A_{g} = A_{\mathrm{c}+1}^{*}$ where $A_{\mathrm{c}+1}^{*}$ is the next step along the Shortest Path. We may prove this assertion as follows: Let

$$\{A_{\mathrm{c},g}\}_{i} \tag{2.32}$$

represent a sequence of locations previously visited by the rat which constitute an unbroken trajectory from the current location to the goal location.

The set, $\Omega_{\mathrm{c},g}$, is the set of all possible trajectories after taking into account all possible paths, short cuts, loops and intersections. So that:

$$\{A_{\mathrm{c},g}\}_{i} \in \Omega_{\mathrm{c},g}, \qquad \Omega_{\mathrm{c},g} \equiv \bigcup_{1}^{n} \{A_{\mathrm{c},g}\}_{i} \tag{2.33}$$

where n represents the total number of possible paths. The number n, will be finite, so long as we only allow forward movement along a finite number of paths. If backward movement is allowed, the n can be infinite. Then we may associate with each sequence $\{A_{\mathrm{c},g}\}_{i} \in \Omega_{\mathrm{c},g}$ a measure of distance:

$$d_{i}(A_{\mathrm{c}}, A_{g}) \tag{2.34}$$

which is simply the number of locations between the current location and the goal location in the i sequence. Note that it is easy to show that this distance measure meets the normal requirements, such as the triangle inequality, that would be required of a measure of distance.

To prove that the navigational mechanism presented in this paper will output the next step along the Shortest Path, we simply need to show that:

$$W_{\mathrm{F}}A_{\mathrm{c}} = W_{\mathrm{B}}^{M-1}A_{g} \tag{2.35}$$

is a necessary and sufficient condition to choose a location that is the next step along the Shortest Path where M is the number of steps in the Shortest Path.

Now we note that:

$$\forall i \in (1,\ldots,n) \qquad d_{i}(A_{\mathrm{c}}, W_{\mathrm{F}}A_{\mathrm{c}}) = 1 \tag{2.36}$$

Because of the possibility of paths that loop back on themselves we may only assert that:

$$d_{i}\left(W_{\mathrm{B}}^{M-k}A_{g}, A_{g}\right) \leq M - k \tag{2.37}$$

For each pathway i, there is a value k. We will consider the pathway $\underset{i}{*}$ which has the minimum value (k) for which:

$$\exists \underset{i}{*} \qquad W_{\mathrm{F}}A_{\mathrm{c}} = W_{\mathrm{B}}^{k}A_{g} \tag{2.38}$$

then it is clear that:

$$d_{\underset{i}{*}}\left(W_{\mathrm{B}}^{k}A_{g}, A_{g}\right) = k \tag{2.39}$$

in which case:

$$d_{\underset{i}{*}}(A_{\mathrm{c}}, A_{g}) = k + 1 \tag{2.40}$$

Moreover it follows that:

$$d_{\underset{i}{*}}(A_{\mathrm{c}}, A_{g}) \leq d_{i}(A_{\mathrm{c}}, A_{g}) \qquad \forall i \neq \underset{i}{*} \;\; i \in (1,\ldots,n) \tag{2.41}$$

To show Eq. (2.41) consider the two possibilities that: (a) no k exists such that condition (2.38) is fulfilled, and (b) the next step along the Shortest Path is a location where condition (2.38) is true for the first time along some path, $\hat{i}$, where $\hat{k} > \min(k)$. Possibility (a) is easy to rule out since if condition (2.38) is never true then no path exists from the current to goal locations (i.e. $\Omega_{\mathrm{cl},g} \equiv \varnothing$). Condition (b) may also be ruled out since in this case:

$$d_{\hat{i}}(A_{\mathrm{c}}, A_{g}) > d_{\underset{i}{*}}(A_{\mathrm{c}}, A_{g}) \tag{2.42}$$

If we assume that we have a location, $A_{\mathrm{c}+1}^{*}$, that is the next step along the Shortest Path, then it is clear that Eq. (2.35) must be true. Otherwise, the Shortest Path would be greater than M steps from the current location, given the assumption that $d_{i}(W_{\mathrm{F}}A_{\mathrm{c}}, W_{\mathrm{B}}^{M-1}A_{g}) > 0 \forall i$.

Moreover, if we expand our consideration to include multiple goal locations then it is clear that the spiking in region CA1 that occurs will represent the next step to the closest goal location since the first matching of input must necessarily take place at $M1$ steps where $M1$ is the shortest number of steps to the closest goal. The shortest paths,

$M2$,$M3$,…,Mn, to all other goals, by definition, are greater than $M1$, and, therefore, matching of input which gives the next step towards the closest goal. Obviously, if there are paths to alternative goals, which are the same length, then spiking in region CA1 will indicate multiple next steps. However, all of these steps are identical in terms of the number of further steps needed to reach a food location. Hence the rat may choose among these goals on a purely random basis with no loss of performance.

3. Role of theta rhythm oscillations

In Section 2, we identified necessary and sufficient conditions for region CA1 to predict the next step along the Shortest Path. In particular, we showed that the activity in region CA1 will predict the next step along the Shortest Path when the activity in this region is described by the equation:

$$\left[W_{\mathrm{CA3}}^{K}A_{\mathrm{c}} + W_{\mathrm{B}}^{M-K}A_{g}\right]_{+} \neq 0, \qquad K = 1 \tag{3.1}$$

However, we have not yet shown in our mechanism why condition (3.1) could be expected to hold. The value $K = 1$ is crucial to getting the next step along the shortest path. As discussed above, there are reasons to worry that $K > 1$ (the Skip Ahead problem) or $K = 0$ (No Next Step) problem.

In addition to the problem of Skip Ahead on retrieval, we also illustrated in Eqs. (2.19) and (2.20) in Section 2 how Skip Ahead can occur during encoding phases. Skip Ahead during encoding can result in the encoding of additional associations between alternative pathways or non-adjacent locations. These associations can generate predictions during retrieval which do not correspond to the next step along the Shortest Path.

In this section, we argue that problems such as Skip Ahead during encoding are eliminated if we assume certain phase relationships for the various signals that we propose are the core of the hippocampal navigational system. Our model of the key synaptic connections in the hippocampal navigational system suggest that certain phase relationships between the synaptic connections may be essential to the operation of this navigational system. Below, we analyze optimal phase relationships for the simple model we have constructed. The purpose of this section is to show optimal phase relationships may be important and to show how such phase relationships may be analyzed from model parameters

To develop the theme of phase relationships, we assume signals into and out of region CA1 are modulated in a periodic fashion. We assume that such modulation takes place on a slower time scale than activity in the region itself. In other words, the neurons in the region may fire many times during a certain phase of modulation of the relevant signals.

Because the electrophysiological data on theta rhythm has been obtained in region CA1, here we will focus on the activation dynamics in region CA1. As part of this focus, we will consider what happens if the W_{F} connections correspond to the Schaffer collaterals projecting from region CA3 to CA1. This avoids the difficulty of ensuring that the spread of activity only goes one step, as Schaffer collaterals do not cause further activity in the presynaptic region CA3 neurons. In contrast to region CA3, region CA1 has very little excitatory recurrent connectivity. If we consider the equation for activity of region CA1 neurons, we can evaluate how performance of the network could depend upon phase relationships of specific variables. In Eq. (2.21), the activation equation for region CA1 was:

$$a_{\mathrm{CA1}} = [a_{\mathrm{CA3}} + a_{\mathrm{ECIII}} - \mu]_{+} = [W_{\mathrm{F}}A_{\mathrm{c}} + W_{\mathrm{B}}^{M-1}A_{g} - \mu]_{+} \tag{3.2}$$

In this section, because we focus on the Schaffer collaterals as W_{F}, we no longer assume that CA3 activity arrives via an identity matrix. Thus, we must consider the flow of activity across these synaptic connections. In addition, we will focus on the changes in somatic membrane potential before thresholding occurs. Therefore, we will use the equation:

$$a_{\mathrm{CA1}} = a_{\mathrm{ECIII}} + W_{\mathrm{F}}a_{\mathrm{CA3}} \tag{3.3}$$

We must now create a continuous time version of this equation. In particular, we include oscillatory functions representing modulatory changes in synaptic currents during theta rhythm, which is consistent with current source density data in region CA1 showing phasic changes in synaptic current at different sets of synaptic connections which are anatomically segregated into different layers of region CA1 (Bragin et al., 1995; Brankack et al., 1993). These changes in synaptic current could be due to both phasic modulation of synaptic strength or phasic modulation of presynaptic spiking activity. Phasic changes in synaptic strength have been demonstrated in experiments showing changes in evoked synaptic potentials in region CA1 on different phases of theta (Rudell and Fox, 1984; Rudell et al., 1980; Wyble, Linster, & Hasselmo, 2000). Phasic changes in presynaptic spiking activity have been observed in both entorhinal cortex (Stewart, Quirk, Barry, & Fox, 1992) and region CA3 (Fox, Wolfson, & Ranck, 1986). For technical reasons, current source density experiments have not been performed in region CA3, but similar phasic changes in synaptic currents could also appear there.

In our description of region CA1 dynamics, we will use oscillatory functions to describe the strength of synaptic currents as well as the membrane potential of the pyramidal cells. We will describe oscillations of the input from entorhinal cortex layer III (which terminate in stratum lacunosum–moleculare) with the function:

$$\theta_{\mathrm{ECIII}}(t) = \left(\frac{X}{2}\sin(\omega t + \phi_{\mathrm{ECIII}}) + \left(1 - \frac{X}{2}\right)\right) \tag{3.4}$$

Oscillations in the synaptic currents from region CA3 to region CA1 (which terminate in stratum radiatum in region

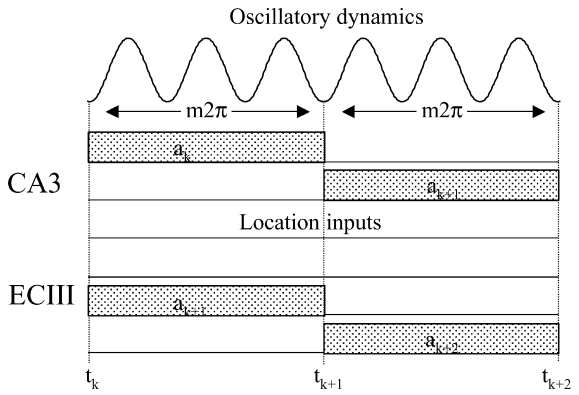

Fig. 5. Summary of the change in discrete location vectors versus continuous time oscillatory functions. At time t_k, the network receives static input of the location vector a_k to region CA3 and the location vector a_{k+1} from entorhinal cortex layer III to region CA1. At time t_{k+1}, the discrete location vectors shift to a static input of location vector a_{k+1} to region CA3 and input of location vector a_{k+2} from entorhinal cortex layer III to region CA1. These static inputs persist over m cycles of the oscillatory functions influencing different components of the network. Thus, the period from t_k to t_{k+1} corresponds to m cycles with total time $m2\pi$.

CA1) will be described with the function:

$$\theta_{\mathrm{CA3}}(t) = \left(\frac{X}{2}\sin(\omega t + \phi_{\mathrm{CA3}}) + \left(1 - \frac{X}{2}\right)\right) \tag{3.5}$$

We also include oscillations in the somatic membrane potential of region CA1 pyramidal cells (in stratum pyramidale of region CA1). This is based on data showing that the excitatory dendritic input is not the only rhythmic input to the soma. The soma also receives rhythmic inhibitory input which causes phasic changes in post-synaptic membrane potential (Fox, 1989; Kamondi, Acsady, Wang, & Buzsaki, 1998). When inhibition is strong, there are strong outward currents (which appear as a current source) and the soma is hyperpolarized. When inhibition is weak, the soma is depolarized and spike generation causes net inward currents (which appear as a current sink). We will represent the effect of this inhibition on the response to synaptic input by multiplying the cell body with an additional oscillatory function:

$$\theta_{\mathrm{somaCA1}}(t) = \left(\frac{X}{2}\sin(\omega t + \phi_{\mathrm{somaCA1}}) + \left(1 - \frac{X}{2}\right)\right) \tag{3.6}$$

With these oscillatory functions, the equation for the somatic membrane potential of region CA1 pyramidal cells takes the form:

$$a_{\mathrm{CA1}}(t) = \theta_{\mathrm{somaCA1}}(t)\{\theta_{\mathrm{ECIII}}(t)a_{\mathrm{ECIII}} + \theta_{\mathrm{CA3}}(t)W_{\mathrm{F}}(t_k)a_{\mathrm{CA3}}\} \tag{3.7}$$

Recall that in Eq. (2.21), the weights within region CA3 were described as:

$$W_{\mathrm{F}} = \sum_{k=1}^{K} a_{k+1}\cdot a_k^{\mathrm{T}} \tag{3.8}$$

Here we will modify this equation to consider the W_{F} weights as the synapses from region CA3 to region CA1.

We will retain the discrete representation of individual locations by activity vectors a_{k} and a_{k+1} which will remain static during a period of time that the animal is in the place field of a cell, as summarized in Fig. 5. We assume these static representations are maintained by an entorhinal buffer, which is supported by data on entorhinal neuronal activity during delay tasks (Young, Otto, Fox, & Eichenbaum, 1997) and has been modeled extensively (Fransen et al., 2002; Jensen and Lisman, 1996; Hasselmo et al., 2002b). This buffer provides sustained spiking of vectors representing the previous location (k) as input from EC layer II to region CA3 as well as the next location ($k + 1$) as input from EC layer III to region CA1. These static location vectors will persist over many cycles of the oscillatory functions, providing stable afferent input during cycles of continuous time oscillations. When a new location $k + 2$ is entered, this becomes the input from ECIII, the location k drops out of the buffer, and the input to region CA3 becomes $k + 1$. Thus, we simplify our analysis by assuming discrete transitions between static states of previous and current location.

We will modify the learning rule equation (3.8) to include oscillatory modulation of the rate of synaptic modification, consistent with physiological data showing rhythmic changes in the induction of long-term potentiation (LTP) on different phases of the theta rhythm (Holscher, Anwyl, & Rowan, 1997; Wyble, Hyman, Goyal, & Hasselmo, 2001). LTP can be induced on the peak of the local theta rhythm in the EEG of stratum radiatum, whereas on the trough of the local EEG, stimulation can cause long-term depression or depotentiation. Thus, we use an oscillating function which goes both positive and negative:

$$\theta_{\mathrm{LTP}} = \sin(\omega t + \phi_{\mathrm{LTP}}) \tag{3.9}$$

As noted above, we designate that the forward connections W_{F} correspond to the Schaffer collaterals from region CA3 to region CA1. We assume that entorhinal buffers provide discrete afferent input vectors representing location k (from entorhinal cortex layer II to region CA3) and location $k + 1$ (from entorhinal cortex layer III to region CA1). Then, Eq. (3.8) can be rewritten as:

$$\frac{dW_{\mathrm{F}}}{dt} = \theta_{LTP}(t)a_{CA1}(t)a^{\mathrm{T}}_{CA3(k)} \tag{3.10}$$

We can insert the activation rule for region CA1, but notice that we do NOT include the effect of the somatic membrane potential, because the modification of synapses depends upon the local dendritic depolarization caused by synaptic input, and does not depend in our model upon the somatic membrane potential.

Because we are describing previous learning to be inserted into the activation rule, we will use the terminology k' to describe the time of previous traversal of the same

location

$$W_F(t_{k'+1}) = \int_{k'}^{k'+1} \theta_{LTP}(t)[\theta_{ECIII}(t)a_{ECIII(k+1)} + \theta_{CA3}(t)W_F(t_{k'})a_{CA3(k)}](a_{CA3(k)})^T dt \quad (3.11)$$

Note that the integration will take place over a period of several cycles during which the discrete location vectors are stable, as shown in Fig. 5. This equation integrates over the time between initial activation of region CA3 by the discrete location vector a_k at time $t_{k'}$ (during which time region CA1 receives the input a_{k+1}) and the termination of vector a_k when region CA3 starts to receive input of the discrete location vector a_{k+1} at time $t_{k'+1}$. The integration will take place over n cycles of oscillation, so the period from k to $k+1$ will be replaced with the interval from 0 to $n2\pi$. For simplicity, we assume that the learning rule does not immediately update the weight matrix. This was used previously (Hasselmo et al., 2002) to allow equations to be evaluated independently. This is consistent with physiological data showing that the effect of activity does not immediately cause LTP, but causes expression of LTP at a later time.

We will be interested to evaluate the effect caused by prior learning of a previous overlapping pathway on learning during exploration of a new pathway. To do this we assume:

$$W_F(t_{k'}) = a_{k+n}a_k^T = a_{ECIII(k+n)}a_{CA3(k)}^T = A_{c+n}A_c^T \quad (3.12)$$

This previous learning could cause problems by contaminating new learning with the reactivation of prior pathways. To determine how the learning rule implemented during the exploration of a pathway influences the subsequent traversal of this pathway, we can plug this Eq. (3.12) (representing previous exploration) into Eq. (3.11), and we can plug the integral in Eq. (3.11) (representing additional exploration) into the activation equation shown in Eq. (3.7) (representing subsequent traversal of the pathway). This gives us:

$$a_{CA1}(t) = \theta_{somaCA1}(t)\theta_{ECIII}(t)a_{ECIII(k+1)} + \theta_{somaCA1}(t)\theta_{CA3}(t) \times \left\{ \int_0^{n2\pi} \theta_{LTP}(t) \left[\theta_{ECIII}(t)a_{ECIII(k+1)} + \theta_{CA3}(t)a_{ECIII(k+n)}a_{CA3(k)}^T a_{CA3(k)} \right] (a_{CA3(k)})^T dt \right\} a_{CA3(k)} \quad (3.13)$$

The activity of the network will be evaluated with a performance measure, which compares the region CA1 activity over a period of time with a vector representing the next desired location A_{c+1}^*. Other possible activity patterns will contribute a negative component to the performance measure. The negative portion of the performance measure is obtained by starting with a vector with all elements set to 1 (vector $\vec{1}$) and subtracting the next desired location vector

$$M = A_{c+1}^{T*} \int_c^{c+1} a_{CA1}(t)dt - (\vec{1} - A_{c+1}^*)^T \int_c^{c+1} a_{CA1}(t)dt \quad (3.14)$$

We can rewrite the performance measure to focus on the problem of no next step (A_c) and the problem of excessive spread onto an undesired alternative pathway (A_{c+n}). In addition, we will integrate over a period of $m2\pi$ cycles between time t_c and t_{c+1}

$$M = A_{c+1}^{T*} \int_0^{m2\pi} a_{CA1}(t)dt - (A_c + A_{c+n})^T \int_0^{m2\pi} a_{CA1}(t)dt \quad (3.15)$$

Now we will assume static inputs of location vectors shown in Eq. (2.21). Thus, the network receives input of A_c from entorhinal cortex layer II to region CA3, so $a_{CA3(k)} = A_c$. The input of A_g from prefrontal cortex to entorhinal cortex layer III causes backward spread which results in retrieval activity $a_{ECIII(k+1)} = W_B^{M-1}A_g = A_{c+1}$. In previous learning stages, region CA3 receives the same input of current location $a_{CA3(k)} = A_c$. In the immediate previous cycles of learning shown in Eq. (3.11), region CA1 receives input from ECIII corresponding to the next desired location $a_{ECIII(k+1)} = A_{c+1}$, but in a previous learning stage shown in Eq. (3.12), the next location was along a different pathway $a_{ECIII(k+n)} = A_{c+n}$. Thus, 3.13 becomes:

$$\int_0^{m2\pi} a_{CA1}(t)dt = \int_0^{m2\pi} \left\{ \theta_{somaCA1}(t)\theta_{ECIII}(t)(A_{c+1}) + \theta_{somaCA1}(t)\theta_{CA3}(t) \left\{ \int_0^{n2\pi} \theta_{LTP}(t) \times \left[\theta_{ECIII}(t)A_{c+1} + \theta_{CA3}(t)A_{c+n}A_c^T A_c \right] \times (A_c)^T dt \right\} A_c \right\} dt \quad (3.16)$$

Now we will insert this integral of region CA1 activity into the performance measure in Eq. (3.15), and we will simplify the various dot products obtained between different vectors

$$M = \left[A_{c+1}^{T*} - (A_c + A_{c+n})^T \right] \int_0^{m2\pi} \left\{ \theta_{somaCA1}(t)\theta_{ECIII}(t) \times (A_{c+1}) + \theta_{somaCA1}(t)\theta_{CA3}(t) \left\{ \int_0^{n2\pi} \theta_{LTP}(t) \times \left[\theta_{ECIII}(t)(A_{c+1}) + \theta_{CA3}(t)A_{c+n}A_c^T A_c \right] (A_c)^T dt \right\} A_c \right\} dt \quad (3.17)$$

With the previous assumption of single active units in each

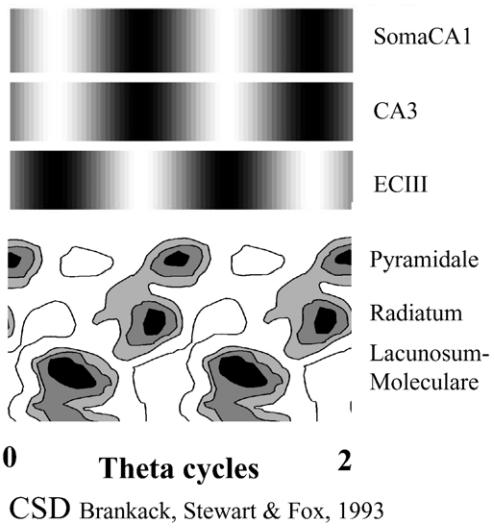

Fig. 6. The best performance in the model occurs with a phase relationship between oscillatory functions which corresponds to the phase relationship between current sinks in different layers of hippocampal region CA1. Top: Plots of oscillatory functions in the model with phases corresponding to best performance: $\phi_{\text{somaCA1}} = 180$, $\phi_{\text{CA3}} = 180$, $\phi_{\text{ECIII}} = 0$. (The LTP function is not shown, but its phase was held at $\phi_{\text{LTP}} = 0$). Bottom: Simplified representation of current source density analysis in fig. 9 from Brankack, Stewart, and Fox (1993). The graph shows current sinks in black (black corresponds to approximately -5 mA/cm^3). Note that the sinks in stratum pyramidale and stratum radiatum occur at similar phase, corresponding to the somaCA1 and CA3 oscillatory functions in the model. The sink in stratum lacunosum–moleculare is out of phase with the other sinks, corresponding to the phase of ECIII input for best performance in the model.

vector, we know that each dot product of a vector with itself will be 1. Thus, $A_c^T A_c = A_{c+1}^T A_{c+1} = 1$, and different vectors will be orthogonal ($A_{c+1}^T A_c = A_{c+n}^T A_{c+1} = 0$). We will also assume that the next step forward from the current location along the desired pathway will match the M-1 input from layer III $A_{c+1}^T W_B^{M-1} A_g = 1$.

This allows simplification of the performance measure to:

$$M = \int_0^{m2\pi} \theta_{\text{somaCA1}}(t)\theta_{\text{ECIII}}(t)\mathrm{d}t + \int_0^{m2\pi} \theta_{\text{somaCA1}}(t)\theta_{\text{CA3}}(t) \times \mathrm{d}t\left\{ \int_0^{n2\pi} \theta_{\text{LTP}}(t)[\theta_{\text{ECIII}}(t)]\mathrm{d}t - \int_0^{n2\pi} \theta_{\text{LTP}}(t)[\theta_{\text{CA3}}(t)]\mathrm{d}t \right\} \tag{3.18}$$

The analytical solution to the lower portion of this equation has been determined previously (Hasselmo et al., 2002a). The analytical solution to the upper portion of the equation can be solved by multiplying the positive-shifted sine waves, making use of a trigonometric identity, and noting that many portions drop out due to integration across full integer cycles

$$\int_0^{m2\pi} \theta_{\text{somaCA1}}(t)\theta_{\text{ECIII}}(t)\mathrm{d}t = (X^2/4)m\pi[\cos(\phi_{\text{somaCA1}} - \phi_{\text{ECIII}}) + m2\pi(1 - X/2)^2 \tag{3.19}$$

Combining these solutions with the solution from the previous article (Hasselmo et al., 2002a) the full Eq. (3.18) becomes:

$$\begin{aligned} M = {} & [(X^2/4)m\pi\cos(\phi_{\text{somaCA1}} - \phi_{\text{ECIII}}) + 2m\pi(1 - X/2)^2] \\ & + [(X^2/4)m\pi\cos(\phi_{\text{somaCA1}} - \phi_{\text{CA3}}) \\ & + 2m\pi(1 - X/2)^2] \\ & \times [(X/2)n\pi\cos(\phi_{\text{LTP}} - \phi_{\text{EC}}) \\ & - (X/2)n\pi\cos(\phi_{\text{LTP}} - \phi_{\text{CA3}})] \end{aligned} \tag{3.20}$$

As shown previously (Hasselmo et al., 2002a), the bottom two lines of this performance measure equation has a maximal positive value for EC in phase with LTP, and 180° out of phase with CA3. The multiplication by a cosine of the difference between somaCA1 and CA3 will be maximal if there is zero phase difference between somaCA1 and CA3. Thus, the portions on the bottom of the Eq. (3.20) require that somaCA1 and CA3 be in phase (0° difference), that LTP and ECIII be in phase (0° difference) and that these two pairs be 180° out of phase (LTP − CA3 = 180). Adding the additional cosine with somaCA1 and ECIII could push the network to have some overlap of somaCA1 and ECIII, but this influence is not sufficiently strong to shift the network from the above requirements. Thus, numerical solution to the equations with $X = m = n = 1$ gives a maximum performance for $\phi_{\text{somaCA1}} = 180, f_{\text{CA3}} = 180$ and $\phi_{\text{ECIII}} = 0$, $\phi_{\text{LTP}} = 0$.

As shown in Fig. 6, these phase relationships of these oscillatory functions for maximal performance correspond to the phase relationships observed in the current source density data from Brankack et al. (1993). The figure shows sine waves corresponding to the phases of maximal function for the oscillations of membrane potential (somaCA1), of synaptic input from region CA3 (CA3) and synaptic input from entorhinal cortex layer III (ECIII). Each of these oscillations corresponds to the inverse of current source density in stratum pyramidale, stratum radiatum and stratum lacunosum–moleculare, because maximal excitatory synaptic input causes strong inward currents (a current sink), and maximum somatic membrane potential will be associated with maximal spiking and inward currents (a current sink). The inverse of these functions has been used for comparison in the figure. The relative phase relationships of the oscillatory functions should correspond to the phase relationships of the current source density data. The experimental data supports these phase relationships, as shown for measurements of currents associated with somatic membrane potential in stratum pyramidale, of currents associated with region CA3 input in stratum radiatum, and currents associated with entorhinal layer III input in stratum lacunosum–moleculare. Thus, the phase relationships derived from the functional framework of this model correspond to the phase relationships observed in the experimental data. If we were to set the threshold so that spiking in region CA1 can only occur when the synaptic

inputs coincide, then this could provide a stronger impetus for some overlap between the CA3 and ECIII input, and the soma currents might be shifted slightly to values between these inputs.

Note that the requirements for separation of the phases of synaptic modification function $\theta_{LTP}(t)$ and the phase of oscillation in synaptic currents $\theta_{CA3}(t)$ across the W_F synapses will become even more important if we consider the effects of the excitatory recurrent connections in region CA3. If we include those connections, we modify Eq. (3.11) to become:

$$W_F(t_{k'+1}) = \int_{k'}^{k'+1} \theta_{LTP}(t)[\theta_{ECIII}(t)a_{ECIII(k+1)} + \theta_{CA3}(t)W_{F(CA3-CA1)}(t_{k'})\theta_{CA3}(t) \times W_{F(CA3)}(t_{k'})a_{CA3(k)}](a_{CA3(k)})^T dt \quad (3.21)$$

This would give dynamics with tremendous potential for causing large scale skip-ahead problems, particularly if the spread of activity in region CA3 is allowed to continue for multiple steps. Thus, the phase relationships derived here for region CA1 should apply similarly to requirements for the phase relationships in region CA3.

3.1. Discussion

Here we have presented a theory of the interaction of hippocampal subregions in regulating goal directed spatial navigation in the rat. This theory involves encoding of associations between neurons in entorhinal cortex layer III and region CA3 representing adjacent spatial locations in the environment. Entorhinal cortical activity reflects the spread from goal backward toward the current location. This then activates the current location representation in entorhinal cortex layer II and region CA3. Activity in region CA3 spreads forward from the current location. The inputs from entorhinal cortex layer III and region CA3 converge in hippocampal region CA1, where co-activated neurons represent the next location in the shortest path to the closest goal location. This selection of shortest pathway is shown analytically in Section 2.

This mechanism for spatial navigation requires changes in functional dynamics, which could be provided by the hippocampal theta rhythm, which is induced by cholinergic and GABAergic input from the medial septum. Section 3 shows how the appropriate encoding and retrieval of pathways in the environment requires rhythmic changes in the relative strength of synaptic currents in region CA1. In particular, as shown previously it is desirable that the rhythmic changes in the strength of synaptic modification (LTP) should be predominantly out of phase with rhythmic changes in the strength of synaptic currents at synapses arising from (CA3). This is consistent with experimental data (Brankack et al., 1993; Holscher et al., 1997; Huerta & Lisman, 1993; Wyble et al., 2001) and with previous analysis of theta rhythm modulation in spatial reversal tasks (Hasselmo et al., 2002a). In addition, input from entorhinal cortex layer II must be maximal at a phase close to the maximal phase of synaptic modification (LTP). As shown in the analysis and in Fig. 6, the membrane potential of region CA1 pyramidal cells should be most depolarized at about the same phase as the strongest currents from region CA3, consistent with experimental current source density data (Brankack et al., 1993).

The network described here would benefit from rhythmic modulation of other parameters, which have not been analyzed in this presentation. In particular, the analysis presented here primarily addresses region CA1 dynamics due to space limitations and the availability of current source density data primarily in region CA1. However, similar effects appear in an analysis of region CA3 dynamics. In addition, these analysis techniques could be extended to address rhythmic changes in activity of neurons in lateral and medial entorhinal cortex layers II and III (Stewart et al., 1992) and in prefrontal cortex. Integrate-and-fire simulations of these mechanisms require input of goal location during the retrieval phase. If prefrontal cortex maintains working memory for goal location, then this region should show spiking activity during the retrieval phase (when CA3 recurrent connections are strong). The focus on the functional role of rhythmic activity could provide a unifying theta theory suitable for addressing the phase relationships of an extensive range of physiological variables.

Acknowledgments

This work was supported by NIH MH61492, NIH MH60013, and NIH MH60450.

References

Amaral, D. G., & Witter, M. P. (1989). The three-dimensional organization of the hippocampal formation: A review of anatomical data. *Neuroscience*, *31*, 571–591.

Andersen, P., Bland, H. B., Myhrer, T., & Schwartzkroin, P. A. (1979). Septo-hippocampal pathway necessary for dentate theta production. *Brain Research*, *165*(1), 13–22.

Barkai, E., & Hasselmo, M. E. (1994). Modulation of the input/output function of rat piriform cortex pyramidal cells. *Journal of Neurophysiology*, *72*(2), 644–658.

Barnes, C. A., McNaughton, B. L., Mizumori, S. J., Leonard, B. W., & Lin, L. H. (1990). Comparison of spatial and temporal characteristics of neuronal activity in sequential stages of hippocampal processing. *Progress in Brain Research*, *83*, 287–300.

Benardo, L. S., & Prince, D. A. (1982). Cholinergic excitation of mammalian hippocampal pyramidal cells. *Brain Research*, *249*(2), 315–331.

Blum, K. I., & Abbott, L. F. (1993). A model of spatial map formation in the hippocampus of the rat. *Neural Computers*, *8*(1), 85–93.

Bragin, A., Jando, G., Nadasdy, Z., Hetke, J., Wise, K., & Buzsaki, G.

(1995). Gamma (40–100 Hz) oscillation in the hippocampus of the behaving rat. *Journal of Neuroscience*, *15*, 47–60.

Brankack, J., Stewart, M., & Fox, S. E. (1993). Current source density analysis of the hippocampal theta rhythm: Associated sustained potentials and candidate synaptic generators. *Brain Research*, *615*(2), 310–327.

Brazhnik, E. S., & Fox, S. E. (1999). Action potentials and relations to the theta rhythm of medial septal neurons in vivo. *Experimental Brain Research*, *127*(3), 244–258.

Bunsey, M., & Eichenbaum, H. (1993). Critical role of the parahippocampal region for paired-associate learning in rats. *Behavioural Neuroscience*, *107*(5), 740–747.

Buzsaki, G., Leung, L. W., & Vanderwolf, C. H. (1983). Cellular bases of hippocampal EEG in the behaving rat. *Brain Research*, *287*(2), 139–171.

Carpenter, G. A., & Grossberg, S. (1993). Normal and amnesic learning, recognition and memory by a neural model of cortico–hippocampal interactions. *Trends in Neuroscience*, *16*(4), 131–137.

DeRosa, E., & Hasselmo, M. E. (2000). Muscarinic cholinergic neuromodulation reduces proactive interference between stored odor memories during associative learning in rats. *Behavourial Neuroscience*, *114*(1), 32–41.

De Rosa, E., Hasselmo, M. E., & Baxter, M. G. (2001). Contribution of the cholinergic basal forebrain to proactive interference from stored odor memories during associative learning in rats. *Behavourial Neuroscience*, *115*(2), 314–327.

Doya, K. (1999). Metalearning, neuromodulation and emotion. In G. Hatano, N. Okada, & H. Tanabe (Eds.), *Affective minds*. New York: Elsevier.

Doya, K. (2002). Metalearning and neuromodulation. *Neural Networks*, *15*(4–5).

Eichenbaum, H., Dudchenko, P., Wood, E., Shapiro, M., & Tanila, H. (1999). The hippocampus, memory, and place cells: Is it spatial memory or a memory space? *Neuron*, *23*(2), 209–226.

Fox, S. E. (1989). Membrane potential and impedence changes in hippocampal pyramidal cells during theta rhythm. *Experimental Brain Research*, *77*, 283–294.

Fox, S. E., Wolfson, S., & Ranck, J. B. J. (1986). Hippocampal theta rhythm and the firing of neurons in walking and urethane anesthetized rats. *Experimental Brain Research*, *62*, 495–508.

Frank, L. M., Brown, E. N., & Wilson, M. (2000). Trajectory encoding in the hippocampus and entorhinal cortex. *Neuron*, *27*(1), 169–178.

Frank, L. M., Brown, E. N., & Wilson, M. A. (2001). A comparison of the firing properties of putative excitatory and inhibitory neurons from ca1 and the entorhinal cortex. *Journal of Neurophysiology*, *86*(4), 2029–2040.

Fransen, E., Alonso, A. A., & Hasselmo, M. E. (2002). Simulations of the role of the muscarinic-activated calcium-sensitive nonspecific cation current I(NCM) in entorhinal neuronal activity during delayed matching tasks. *Journal of Neuroscience*, *22*(3), 1081–1097.

Ghoneim, M. M., & Mewaldt, S. P. (1975). Effects of diazepam and scopolamine on storage, retrieval and organizational processes in memory. *Psychopharmacologia*, *44*, 257–262.

Hasselmo, M. E. (1995). Neuromodulation and cortical function: Modeling the physiological basis of behavior. *Behavourial Brain Research*, *67*, 1–27.

Hasselmo, M. E. (1999). Neuromodulation: Acetylcholine and memory consolidation. *Trends in Cognitive Sciences*, *3*, 351–359.

Hasselmo, M. E., & Barkai, E. (1995). Cholinergic modulation of activity-dependent synaptic plasticity in rat piriform cortex. *Journal of Neuroscience*, *15*(10), 6592–6604.

Hasselmo, M. E., & Bower, J. M. (1993). Acetylcholine and memory. *Trends in Neuroscience*, *16*(6), 218–222.

Hasselmo, M. E., & Fehlau, B. P. (2001). Differences in time course of cholinergic and GABAergic modulation of excitatory synaptic potentials in rat hippocampal slice preparations. *Journal of Neurophysiology*, *86*, 1792–1802.

Hasselmo, M. E., & Schnell, E. (1994). Laminar selectivity of the cholinergic suppression of synaptic transmission in rat hippocampal region CA1: Computational modeling and brain slice physiology. *Journal of Neuroscience*, *14*(6), 3898–3914.

Hasselmo, M. E., & Wyble, B. P. (1997). Simulation of the effects of scopolamine on free recall and recognition in a network model of the hippocampus. *Behavourial Brain Research*, *89*, 1–34.

Hasselmo, M. E., Bodelon, C., & Wyble, B. P. (2002a). A proposed function for hippocampal theta rhythm: Separate phases of encoding and retrieval enhance reversal of prior learning. *Neural Computation*, *14*(4), 793–817.

Hasselmo, M. E., Cannon, R. C., & Koene, R. A. (2002b). A simulation of parahippocampal and hippocampal structures guiding spatial navigation of a virtual rat in a virtual environment: A functional framework for theta theory. In M. P. Witter, & F. G. Wouterlood (Eds.), *The parahippocampal region: Organisation and role in cognitive functions*. Oxford: Oxford University Press.

Holscher, C., Anwyl, R., & Rowan, M. J. (1997). Stimulation on the positive phase of hippocampal theta rhythm induces long-term potentiation that can Be depotentiated by stimulation on the negative phase in area CA1 in vivo. *Journal of Neuroscience*, *17*(16), 6470–6477.

Huerta, P. T., & Lisman, J. E. (1993). Heightened synaptic plasticity of hippocampal CA1 neurons during a cholinergically induced rhythmic state. *Nature*, *364*, 723–725.

Jensen, O., & Lisman, J. E. (1996). Novel lists of 7 + /− 2 known items can be reliably stored in an oscillatory short-term memory network: Interaction with long-term memory. *Learning and Memory*, *3*(2-3), 257–263.

Johnston, D., & Amaral, D. G. (1998). Hippocampus. In G. M. Shepherd (Ed.), *Synaptic organization of the brain* (pp. 417–458). London: Oxford University Press.

Kali, S., & Dayan, P. (2000). The involvement of recurrent connections in area CA3 in establishing the properties of place fields: A model. *Journal of Neuroscience*, *20*(19), 7463–7477.

Kamondi, A., Acsady, L., Wang, X. J., & Buzsaki, G. (1998). Theta oscillations in somata and dendrites of hippocampal pyramidal cells in vivo: Activity-dependent phase-precession of action potentials. *Hippocampus*, *8*(3), 244–261.

Lee, M. G., Chrobak, J. J., Sik, A., Wiley, R. G., & Buzsaki, G. (1994). Hippocampal theta activity following selective lesion of the septal cholinergic system. *Neuroscience*, *62*(4), 1033–1047.

Levy, W. B. (1996). A sequence predicting CA3 is a flexible associator that learns and uses context to solve hippocampal-like tasks. *Hippocampus*, *6*, 579–590.

Levy, W. B., & Steward, O. (1983). Temporal contiguity requirements for long-term associative potentiation/depression in the hippocampus. *Neuroscience*, *8*(4), 791–797.

Linster, C., & Hasselmo, M. E. (2001). Neuromodulation and the functional dynamics of piriform cortex. *Chemical Senses*, *26*, 585–594.

Linster, C., Garcia, P. A., Hasselmo, M. E., & Baxter, M. G. (2001). Selective loss of cholinergic neurons projecting to the olfactory system increases perceptual generalization between similar, but not dissimilar, odorants. *Behavioural Neuroscience*, *115*(4), 826–833.

Markus, E. J., Qin, Y. L., Leonard, B., Skaggs, W. E., McNaughton, B. L., & Barnes, C. A. (1995). Interactions between location and task affect the spatial and directional firing of hippocampal neurons. *Journal of Neuroscience*, *15*(11), 7079–7094.

Marrosu, F., Portas, C., Mascia, M. S., Casu, M. A., Fa, M., Giagheddu, M., Imperato, A., & Gessa, G. L. (1995). Microdialysis measurement of cortical and hippocampal acetylcholine release during sleep-wake cycle in freely moving cats. *Brain Research*, *671*(2), 329–332.

McNaughton, B. L., Barnes, C. A., & O'Keefe, J. (1983). The contributions of position, direction, and velocity to single unit activity in the hippocampus of freely-moving rats. *Experimental Brain Research*, *52*(1), 41–49.

Mehta, M. R., Barnes, C. A., & McNaughton, B. L. (1997). Experience-dependent, asymmetric expansion of hippocampal place fields.

Proceedings of the National Academy of Sciences, United States of America, *94*(16), 8918–8921.

M'Harzi, M., Palacios, A., Monmaur, P., Willig, F., Houcine, O., & Delacour, J. (1987). Effects of selective lesions of fimbria-fornix on learning set in the rat. *Physiology and Behaviour*, *40*, 181–188.

Muller, R. U., & Kubie, J. L. (1989). The firing of hippocampal place cells predicts the future position of freely moving rats. *Journal of Neuroscience*, *9*, 4101–4110.

Muller, R. U., & Stead, M. (1996). Hippocampal place cells connected by Hebbian synapses can solve spatial problems. *Hippocampus*, *6*(6), 709–719.

Numan, R., Feloney, M. P., Pham, K. H., & Tieber, L. M. (1995). Effects of medial septal lesions on an operant go/no-go delayed response alternation task in rats. *Physiology and Behaviour*, *58*, 1263–1271.

O'Keefe, J., & Recce, M. L. (1993). Phase relationship between hippocampal place units and the EEG theta rhythm. *Hippocampus*, *3*, 317–330.

Patil, M. M., & Hasselmo, M. E. (1999). Modulation of inhibitory synaptic potentials in the piriform cortex. *Journal of Neurophysiology*, *81*(5), 2103–2118.

Patil, M. M., Linster, C., Lubenov, E., & Hasselmo, M. E. (1998). Cholinergic agonist carbachol enables associative long-term potentiation in piriform cortex slices. *Journal of Neurophysiology*, *80*, 2467–2474.

Quirk, G. J., Muller, R. U., Kubie, J. L., & Ranck, J. B., Jr (1992). The positional firing properties of medial entorhinal neurons: Description and comparison with hippocampal place cells. *Jounal of Neuroscience*, *12*(5), 1945–1963.

Rawlins, J. N., Feldon, J., & Gray, J. A. (1979). Septo-hippocampal connections and the hippocampal theta rhythm. *Experimental Brain Research*, *37*(1), 49–63.

Rudell, A. P., & Fox, S. E. (1984). Hippocampal excitability related to the phase of the theta rhythm in urethanized rats. *Brain Research*, *294*, 350–353.

Rudell, A. P., Fox, S. E., & Ranck, J. B. J. (1980). Hippocampal excitability phase-locked to the theta rhythm in walking rats. *Experimental Neurology*, *68*, 87–96.

Samsonovich, A., & McNaughton, B. L. (1997). Path integration and cognitive mapping in a continuous attractor neural network model. *Journal of Neuroscience*, *17*(15), 5900–5920.

Shepherd, G. M. (1998). *The synaptic organization of the brain*. New York: Oxford University Press.

Skaggs, W. E., McNaughton, B. L., Wilson, M. A., & Barnes, C. A. (1996). Theta phase precession in hippocampal neuronal populations and the compression of temporal sequences. *Hippocampus*, *6*, 149–172.

Stewart, M., & Fox, S. E. (1990). Do septal neurons pace the hippocampal theta rhythm? *Trends in Neuroscience*, *13*(5), 163–168.

Stewart, M., Quirk, G. J., Barry, M., & Fox, S. E. (1992). Firing relations of medial entorhinal neurons to the hippocampal theta rhythm in urethane anesthetized and walking rats. *Experimental Brain Research*, *90*(1), 21–28.

Sutherland, R. J., Whishaw, I. Q., & Regehr, J. C. (1982). Cholinergic receptor blockade impairs spatial localization by use of distal cues in the rat. *Journal of Comparitive Physiology and Psychology*, *96*(4), 563–573.

Sutton, R. S., & Barto, A. G. (1998). *Reinforcement learning (adaptive computation and machine learning)*. Cambrige, MA: MIT Press.

Whishaw, I. Q., & Tomie, J. A. (1997). Perseveration on place reversals in spatial swimming pool tasks: Further evidence for place learning in hippocampal rats. *Hippocampus*, *7*(4), 361–370.

Wyble, B. P., Linster, C., & Hasselmo, M. E. (2000). Size of CA1-evoked synaptic potentials is related to theta rhythm phase in rat hippocampus. *Journal of Neurophysiology*, *83*(4), 2138–2144.

Wyble, B. P., Hyman, J. M., Goyal, V., & Hasselmo, M. E. (2001). Phasic relationship of LTP induction and behavior to the theta rhythm in the rat hippocampus. *Society of Neuroscience Abstracts*, *27*, 53719.

Young, B. J., Otto, T., Fox, G. D., & Eichenbaum, H. (1997). Memory representation within the parahippocampal region. *Journal of Neuroscience*, *17*(13), 5183–5195.

Yu, A. J., & Dayan, P. (2002). Acetylcholine and cortical inference. *Neural Networks*, *15*(4–5).